Theoretical Studies on Dications and Tricications of FH, ClH, and BrH. Properties of the Bound $1^5\Sigma^-$ States. Electron-Spin *g*-Factors and Fine/Hyperfine Constants of the Metastable $X^3\Sigma^-$ States of ClH^{2+} and BrH^{2+}

Pablo J. Bruna and Friedrich Grein*

Department of Chemistry and Centre for Laser, Atomic and Molecular Sciences, University of New Brunswick, Fredericton, New Brunswick, Canada E3B 6E2

Received: December 13, 2005; In Final Form: February 14, 2006

This theoretical study reports calculations on the fine and hyperfine structure parameters of the metastable $X^3\Sigma^-(\sigma^2\pi^2)$ state of ClH^{2+} and BrH^{2+}. Data on the repulsive FH^{2+} system are also included for comparison purposes. The hyperfine structure (hfs) coupling constants for magnetic (A_{iso}, A_{dip}) and quadrupole (eQq) interactions are evaluated using B3LYP, MP4SDQ, CCSD, and QCISD methods and several basis sets. The fine structure (fs) constants (zero-field splitting λ and spin-rotation coupling γ) and electron-spin magnetic moments (*g*-factor) are evaluated in 2nd-order perturbation theory using multireference CI (MRCI) wave functions. Our calculations find for ^{35}Cl of ClH^{2+} $A_{iso}/A_{dip} = 110/-86$ MHz; $eQq_0 = -59$ MHz; $2\lambda = 20.4$ cm^{-1}; $g_\perp(v = 0) = 2.02217$; and $\gamma = -0.31$ cm^{-1} (to be compared with the available experimental A_{iso}/A_{dip}= 162/-30 MHz). For $^{79}BrH^{2+}$, the corresponding values are 300/−400 MHz; 368 MHz; 362.6 cm^{-1}; 2.07302; and −0.98 cm^{-1} (experimental $2\lambda = 445(\pm 80)$ cm^{-1}). We find $g_\perp(ClH^{2+})$ to increase by about 0.0054 between $v = 0$ and 2, whereas the experimental effective $g_\perp$ changes drastically with vibrational excitation. Nuclear quadrupole coupling constants for halogen atoms X are found to be as large as corresponding $A_{dip}(X)$'s, indicating that both terms may have to be included in the Hamiltonian used to interpret XH^{2+} hyperfine spectra. A novel finding relates to the bound character of the $1^5\Sigma^-(\sigma\pi^2\sigma^*)$ state in FH^{2+}, as already known for ClH^{2+} and BrH^{2+}, but having a deeper potential well $D_e \approx 4000$ cm^{-1} (versus 1000 cm^{-1} in the heavier radicals). Vertical ionization potentials for formation of XH^{3+} tricications are also discussed.

1. Introduction

During the last two decades, the study of double-positive diatomic hydrides, XH^{2+}, has been the topic of numerous experimental and theoretical publications. To date, however, experimental works[1] have provided information mainly about energetics (via ionization potentials (IP) or kinetic energy releases (KER)) and less about the properties of metastable states (geometries, vibrational/rotational constants, charge-(spin)-density distributions, etc.). Such an unfavorable situation relates to three major drawbacks generally affecting XY^{2+} ions: (a) extremely low densities in laboratory formed species (10^2-10^6 cm^{-3} vs 10^{19} cm^{-3} for gases at atmospheric pressure); (b) high reactivity (very short lifetimes due to unimolecular decompositions and/or environmental interactions); and (c) few XY^{2+} potentials have local minima. Not surprisingly, high-resolution, rotationally resolved spectra have only been reported for N_2^{2+}, NO^{2+}, ClD^{2+}, and hyperfine structure (hfs), and electron-spin *g*-factors are known for just one of them (ClD^{2+}).[2] The zero-field splitting (zfs) for $X^3\Sigma^-$ of BrH^{2+}/BrD^{2+} has been measured in three different double-ionization studies,[3a−3c] making them the only XH^{2+} species for which fine structure (fs) data are experimentally available.

The hyperfine/Zeeman spectra of $^{35,37}ClD^{2+}$ have been partially assigned.[4,5] Two fs parameters were, and still are, unknown, the zfs constant λ and spin-rotation constant γ, making the assignments with assumed λ and γ values questionable. Also unknown remain nuclear quadrupole contributions. Optical spectroscopy, electronic excitation from $X^3\Sigma^-$, is of no use since transitions into $1^1\Delta$ and $1^1\Sigma^+$ are forbidden, whereas allowed triplet−triplet transitions involve upper states of repulsive character.

A metastable XH^{2+} state is assumed to arise by the interaction between attrative (X^{2+}+H) and repulsive (X^++H^+) channels.[6] As discussed elsewhere,[7,8] the parameter $\Delta IP = [IP(X^+) - IP(H)]$ indicates the possible existence of metastable states: the closer $IP(X^+)$ is to 13.605 eV the more stable is XH^{2+}. In the XH^{2+} series (X= F, Cl, Br), the corresponding ΔIP's are 21.4, 10.2, and 8.0 eV.[9] The $\Delta IP(FH^{2+})$ value is prohibitively large to induce stability, and all known FH^{2+} potentials are repulsive.[10,11] That is not the case for ClH^{2+} and BrH^{2+}, each having one bound ($1^5\Sigma^-$) and three metastable states ($X^3\Sigma^-$, $1^1\Delta$, $1^1\Sigma^+$).[12−22] Considering the first three rows of the periodic table, ΔIP amounts to ca. 11−21 eV from B to F, 3−10 eV from Al to Cl, and 2.5−8 eV from Ga to Br.[9] They support the experimental observation that B to F (Ne) do not generate metastable XH^{2+} ions, whereas atoms from higher rows do.[6−8]

Ab initio studies on dications are important not only because they give insight about potential barriers, tunneling lifetimes, etc. in metastable states[14−17,20] but they are also crucial for interpreting experimental data for repulsive states.[12,13] A literature survey reveals that such studies have focused on standard spectroscopic properties for metastable states (geometries, vibrational frequencies, etc.), whereas calculations of hf/hfs parameters or electron-spin *g*-factors/rotational coupling constants are practically nonexistent, except for the *g*-factors of BeH^{2+} [23] and $X^3\Sigma^-$ zfs data for ClH^{2+}/BrH^{2+}.[16,17]

* Corresponding author. Fax: +1-506-453-4981. E-mail: fritz@unb.ca.

10.1021/jp0572838 CCC: $33.50
Published on Web 03/18/2006

The main goal of this study is to evaluate the fs and hfs parameters, and the magnetic moments (*g*-factors), for the $X^3\Sigma^-$ ground states (GS) of ClH^{2+} and BrH^{2+}. It will also shed some light on the bonding features of XH^{2+}. Formation of a metastable $X^3\Sigma^-$ minimum implies that some amount of electron-density has been transferred from X^+ to H^+ in order to overcome their mutual Coulomb repulsion. Most importantly, the mixing between (X^++H^+) and (X^{2+}+H) structures should be seen in the hf parameters of each nucleus, which offer the opportunity of quantifying the relative weight of both structures, in particular the amount of charge density at the H center. Previous studies[12−15] found $1^5\Sigma^-(\sigma\pi^2\sigma^*)$ of ClH^{2+} and BrH^{2+} to be bound, whereas others[10,11,18h] were interested in the IPs for XH^{3+} ions. The stabilities of $1^5\Sigma^-$ in FH^{2+} and of all three trications will also be investigated here.

2. Technical Details

The hyperfine coupling constants (hfccs) and nuclear quadrupole coupling constants (nqccs) are calculated using the spin- and charge-density distributions (SDD and CDD) provided by Gaussian 03 (G03)[24] by means of spin-unrestricted ab initio (MP4SDQ, CISD, CCSD, QCISD) and density-functional theory (DFT) procedures (B3LYP, B3PW91). Different basis sets were used, e.g., Pople's 6-31++G(2df,2pd) and Dunning's aug-cc-pVTZ/pVQZ. For brevity, we only report here the median value of the various hfs parameters. Matrix elements of SO (spin−orbit) and L (electronic angular momentum) operators are evaluated with multireference CI wave functions (MRDCI)[25] and 6-311++G(2d,2pd) basis sets. The SO matrix elements include all one- and two-electron terms from a Breit-Pauli Hamiltonian.[26] The CI calculations on XH^{2+} are carried out in C_{2v} symmetry, mostly using spin-restricted $X^3\Sigma^-(\sigma^2\pi^2)$ SCF-MOs. Those on $1^5\Sigma^-(\sigma\pi^2\sigma^*)$ states, however, are based on parent MOs. The accuracy of SO improves if inner shells are also correlated.[27,28] In line with this, ClH^{2+} and BrH^{2+} were studied correlating 12 and 22 electrons, respectively ($1s^22s^2$ frozen core for Cl and $1s^22s^22p^63s^2$ for Br). The FH^{2+} calculations correlate 6 valence electrons (VE), with $1s^2$(F) kept frozen. The *L* values correspond to the origin of coordinates placed at the electronic charge centroid.[29] Unless specified otherwise, SO and *L* values cited in the text and tables are for the Cartesian representation.

3. Results

The results below include (i) relative energies for XH^{n+} ions (section 3.1); (ii) magnetic/electric hfs parameters from G03 calculations (3.2 and 3.3); and (iii) fs data and *g*-factors at the MRDCI level (3.4 and 3.5). A prior theoretical study[28] on FH^+, ClH^+, and BrH^+ reproduced quite well the corresponding experimental fs/hfs data, and the same is expected here for the lesser known XH^{2+} dications.

3.1. Relative Stabilities and Energies. Diatomic (XY) potential curves are (a) stable, or bound, if there is at least one local minimum $E_m(R_e)$ at the equilibrium distance $R_e \ll R = \infty$ and it lies below the (X+Y) products; (b) metastable, as in case (a) but with $E_m(R_e)$ lying above (X+Y); and (c) unstable, or repulsive, if the only minimum is at $E(R = \infty)$. Practically all states of a dication are repulsive and very few may be metastable (the existence of just one already becomes relevant). Exceptionally, the GS is bound, e.g., $CaH^{2+}(X^2\Sigma^+)$ with 1 valence electron (VE).[8] See ref 1 for several examples of dicationic potential surfaces.

ClH^{2+} and BrH^{2+} have one bound ($1^5\Sigma^-$) and three metastable states each ($X^3\Sigma^-$, $1^1\Delta$, $1^1\Sigma^+$), a remarkably high stability for an hydride, but FH^{2+} apparently has none.[10−20] Experimental studies suggest that $g(ClH^{2+})$ strongly depends on *R*, and to test the validity of such statement, we have calculated the low-lying potential curves of ClH^{2+}, which are displayed in Figure 1 (they look alike to those in the literature refs 12, 14, 20, and 22). It also came to our attention that two experimental spectra, one on FH (Auger[10a]) and the other on ClH (electron-impact[18h]), dealt briefly with triply ionized XH^{3+}, for which theoretical data are scarce (see below). For the sake of completeness, vertical IPs from XH into XH^+, XH^{2+}, and XH^{3+} will be calculated as well.

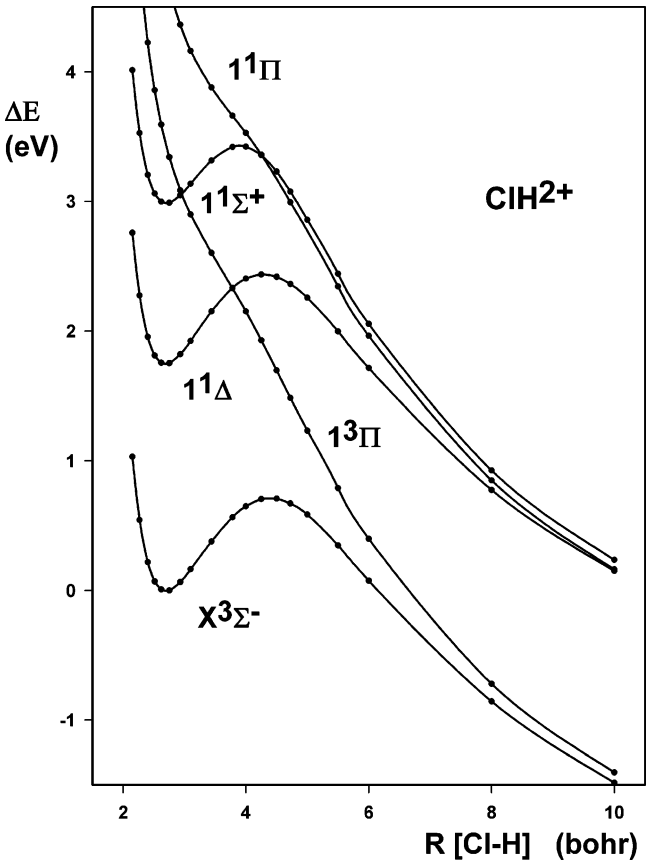

Figure 1. Potential curves for low-lying electronic states of ClH^{2+} (MRDCI, correlating 6 electrons).

3.1.1. XH^{2+} Vertical Excitation Energies. Table 1 lists vertical excitation energies (ΔE_v) for low-lying XH^{2+} states, along with published data. For FH^{2+}, we use $R = 2.20$ bohr, which lies between 1.9 bohr for $X^2\Pi$ and 2.3 bohr for $A^2\Sigma^+$ in FH^+ (NB: $R_e = 1.73$ bohr for the GS of FH is much shorter).[30] The $R_e(X^3\Sigma^-)$'s for ClH^{2+} and BrH^{2+} (Table 1) are those reported in previous optimizations.[12−15,20b]

The ΔE_v's of ClH^{2+}/BrH^{2+} show a common ordering $X^3\Sigma^- < 1^1\Delta < 1^1\Sigma^+ < 1^3\Pi < 1^1\Pi < 2^1\Sigma^+$, or $\sigma^2\pi^2 < \sigma\pi^3 < \pi^4$ in terms of configurations. Corresponding ΔE_v values differ by no more than 0.5 eV. The state sequence is different in FH^{2+} [two triplets below all singlets] but agrees with that expected for (F^++H^+) products, where the $F^+(s^2p^4)$ states follow the ordering $^3P(X^3\Sigma^-, 1^3\Pi) < {}^1D(1^1\Sigma^+, 1^1\Pi, 1^1\Delta) < {}^1S(2^1\Sigma^+)$, with correlating XH^{2+} states in parentheses. Although Cl^+/Br^+ certainly has the same state pattern as F^+, stabilizing effects operating in ClH^{2+} and BrH^{2+} but not in FH^{2+}, due to mixings with $X^{2+}(^4S < {}^2D < {}^2P) + H(^2S)$, are ultimately responsible for the stability differences at short *R*.

All theoretical studies find similar ΔE_v's (Table 1). Most of them focused on XH → XH^{2+} ionization, and therefore

TABLE 1: Vertical Excitation Energies ΔE_v (eV) Relative to $X^3\Sigma^-(\sigma^2\pi^2)$ for Relevant XH^{2+} States (X = F, Cl, and Br), and Comparison with Literature Data[a]

XH^{2+}	refs	$1^1\Delta$ ($\sigma^2\pi^2$)	$1^1\Sigma^+$ ($\sigma^2\pi^2$)	$1^3\Pi$ ($\sigma\pi^3$)	$1^1\Pi$ ($\sigma\pi^3$)	$2^1\Sigma^+$ (π^4)	$1^5\Sigma^-$ ($\sigma\pi^2\sigma^*$)
FH^{2+}	tw	2.86	4.39	2.29	4.92	8.61	17.33
	11c[b]	2.95	5.84	3.35	6.37	11.33	
	11d[c]	2.73	5.47	3.16	6.02	10.74	
	11e[d]	3.00	4.60	3.40	6.30	11.20	
expt.	10[e]	(0.00)	(1.93)			(7.36)	
ClH^{2+}	tw	1.72	2.96	3.32	4.66	9.11	9.34
	18a	1.74	2.99	4.00	6.71		
	18b	1.80	3.00	3.90	5.50	10.60	
	20a[f]	1.72		3.87			
	12 and 14[g]	1.54	2.84	3.86	5.26	10.24	≈10.5
	20b[h]	1.52	2.85	3.19			
	16a[i]	1.78	3.12	3.86	5.44	10.57	
expt.	12[j]	1.50	2.70		5.00	9.60	
	18d	1.62	2.77				
	18e	1.49	2.75				
BrH^{2+}	tw	1.58	2.76	3.52	4.65	9.60	8.15
	13 and 15[k]	1.62	2.57	3.87	4.97	10.10	9.72
	17[l]	1.68	2.94	2.48			
expt.	19b[m]	1.47	2.70	2.57			
expt.	3[n]	1.10	2.40				
		1.36	2.62				

[a] tw = this work. MRDCI data at $R(X^3\Sigma^-)$'s [bohr] of 2.200 (FH^{2+}), 2.752 (ClH^{2+}) and 2.954 (BrH^{2+}). Corresponding $X^3\Sigma^-$ energies [au]: −98.5047 (6 e's); −459.0485 (12 e's) and −2572.1910 (22 e's). [b] HF/STO, R^F= 1.7329 bohr (FH GS). [c] Spin-adapted HF, R^F. [d] Direct MRDCI, R^F. [e] Auger spectrum (triplets not detected). [f] CASSCF−CI, R^{Cl}= 2.409 bohr (ClH GS). [g] MRDCI, R^{Cl}. [h] CASSCF-MRDCI, R = 2.74 bohr. [i] Relativistic CI; $^3\Pi_{0-}$ and $^1\Delta_2$ sublevels relative to lowest $^3\Sigma_1^-$ (all v = 0 data). [j] Double-charge-transfer spectrum. TPEsCO spectrum[18g] finds 1.49/2.75 eV for $1^1\Delta/1^1\Sigma^+$. [k] MRDCI [nonrelativistic, R^{Br} = 2.66 bohr (BrH)]. Adiabatic ΔE's for $1^1\Delta/1^1\Sigma^+$: (i) 1.19/2.61 eV [nonrelativistic, $R(X^3\Sigma^-)$ = 2.71 bohr]; and (ii) 1.57/2.67 eV [relativistic, R = 2.69 bohr]. [l] Relativistic results (1st entry: Dirac−Fock; 2nd: MRCI), for $^3\Pi_2$, $^1\Delta_2$, and $^1\Sigma_0^+$ sublevels relative to $^3\Sigma_{0+}^-$(all v=0 data). The $^3\Pi_{0-}$ sublevel lies at 3.47 eV (DF) or 3.28 eV (MRCI). [m] Auger spectrum, difference between adiabatic (double-ionization) IP's. [n] Auger spectrum, energies relatives to $^3\Sigma_0^-$ sublevel.

TABLE 2: Relative Energy (ΔE_d) to Dissociation Products I−III, Stabilization Energy (ΔE_{el}) and ΔIP Parameter for Low-Lying Electronic States of XH^{2+} (X = F, Cl, and Br)[a,b]

	FH^{2+}			ClH^{2+}			BrH^{2+}		
state[c,d]	$-\Delta E_d$	ΔE_{el}	ΔIP[e]	$-\Delta E_d$	ΔE_{el}	ΔIP[e]	$-\Delta E_d$ [f]	ΔE_{el}	ΔIP[e]
$X^3\Sigma^-(\sigma^2\pi^2)$ I(a)	8.98	3.39	21.4	4.26	5.63	10.2	2.98	6.23	8.0
	(9.78)	(2.52)		(4.60)	(5.09)		(3.69)	(5.36)	
$1^3\Pi(\sigma\pi^3)$ I(b)	11.28	1.09	25.6	7.58	2.31	12.4	6.50	2.71	9.9
$1^1\Delta(\sigma^2\pi^2)$ II(b)	9.12	3.25	23.0	4.37	5.52	11.1	3.08	6.13	8.9
$1^1\Sigma^+(\sigma^2\pi^2)$ II(c)	10.65	1.72	23.0	5.60	4.29	11.1	4.26	4.95	8.9
$1^1\Pi(\sigma\pi^3)$ II(b)	11.18	1.19	25.2	7.30	2.59	12.5	6.15	3.06	10.4
$2^1\Sigma^+(\sigma^2\pi^2)$ III(m)	11.99	0.38	>40	9.87	0.02	>25	9.34	−0.13	>22

[a] MRDCI Data, in eV. $\Delta E_d(R) = [E(\infty) - E(R)]$, where $E(\infty)$ stands for the energy of corresponding dissociation channel. ΔE_d is D_e for metastable and KER for repulsive states. R distances as in Table 1 (tw). Values in parentheses are derived using CID data from ref 33 (see text). [b] $\Delta E_{el}(R) = [1/R + \Delta E_d(R)]$, electronic stabilization energy relative to $1/R$ potential. [c] Channels I < II < III: $X^+(s^2p^4)$ states $^3P < ^1D < ^1S$, $+H^+$. Ch. $a < b < c$: $X^{2+}(s^2p^3)$ states $^4S < ^2D < ^2P$, +H. Channel m: $[X^{2+}(M) + H(^2S)]$, where M is $^2D(sp^4)$ for F^{2+}, and $s^2p^2d/s^2p^2s_{Ryd}$ for Cl^{2+} and Br^{2+}.[9] [d] I(a) indicates that I (repulsive) and a (attractive) generate a $^3\Sigma^-$ state each. Similarly, II(c) shows that $1^1\Sigma^+$ is generated by II, and $2^1\Sigma^+$ by c, etc. [e] ΔIP = [IP(X^+) − IP(H)], where IP(X^+) involves X^+/X^{2+} states generating in a given type of electronic state, e.g., ΔIP for $1^1\Sigma^+$ [II(c)] stands for $E[X^{2+}(^2P) + H] - E[X^+(^1D) + H^+]$. Experimental data.[9] Note that listed asymptotic $\Delta IP(R = \infty)$'s are about 6.8 eV (=1/R) smaller at R = 4 bohr, for example. [f] $-\Delta E_d$ (KER) of 6.78 eV for $1^3\Pi$, 6.42 eV for $1^1\Pi$ (calc.) and 6.84 eV for $1^{3,1}\Pi$ (expt.).[12] Our values are slightly smaller because $R_e(X^3\Sigma^-)$ was used.

$R_e(X^1\Sigma^+)$ of XH was used for reporting $\Delta E_v(XH^{2+})$'s. Accordingly, our results at $R_e(X^3\Sigma^-)$'s show some discrepancies with previous data, which are minor for ClH^{2+}/BrH^{2+} but larger for FH^{2+} because R = 2.2 bohr used here is 0.5 bohr longer than in the GS of FH.[30] Experimentally, the FH Auger spectra[10] were assigned to three FH^{2+} singlet states ($1^1\Delta$ and $1,2^1\Sigma^+$), with the lowest $1^3\Sigma^-$, $1^3\Pi$ states remaining undetected. For this reason, the experimental ΔE_v's are relative to $1^1\Delta$ of FH^{2+} (data in parentheses, Table 1). A measured ΔE_v of 1.93 eV between the $\sigma^2\pi^2$ states $1^1\Delta - 1^1\Sigma^+$ (Table 1) is in moderate agreement with MRDCI results (1.53 and 1.60 eV).

3.1.2. Relative Stabilities of Triplets and Singlets. Metastable XY^{2+} potentials can be characterized via the parameters T_e, R_e, ω_e, B_e, D_e, etc., as done for bound states, plus the IPs with respect to XY or XY^+. For repulsive XY^{2+} potentials, solely IP data can be given. However, all states can be described in the same footing by specifying the energy $E(R)$ of a particular XY^{2+} potential at distance R relative to two reference energies: (i) $E(R = \infty)$, the energy at dissociation and (ii) $V_{Coul} = 1/R$, the repulsive Coulomb potential between two positive charges. For this purpose, we define $\Delta E_d(R) = [E(\infty) - E(R)]$ and $\Delta E_{el}(R) = [1/R + \Delta E_d(R)] = [1/R + E(\infty) - E(R)]$. Here, $E(\infty)$ is via MRDCI data for $(X^+ + H^+)$ at R = 200 bohr, and their total energies shifted down by $-1/R = -0.005$ au.

Table 2 summarizes the parameters ΔE_d, ΔE_{el}, and ΔIP = [IP(X^+) − IP(H)] characterizing the lowest six XH^{2+} states generated by the atomic states $^3P(I) < ^1D(II) < ^1S(III)$ of $X^+(s^2p^4)$,[9] plus H^+. As stated before, channel I correlates with $1(X)^3\Sigma^-, 1^3\Pi$ of XH^{2+}, channel II gives rise to $1^1\Delta$, $1^1\Pi$, $1^1\Sigma^+$, and channel III correlates with $2^1\Sigma^+$. Further, the attractive channels (X^{2+}+H) labeled a, b and c, respectively, combine the $X^{2+}(s^2p^3)$ states $^4S < ^2D < ^2P$ with $H(^2S)$.[9] The XH^{2+} states

generated by them are channel a $\underline{2^3\Sigma^-}$ and $1^5\Sigma^-$; channel b $\underline{2^1\Delta}$, $\underline{2^3\Pi}$, $\underline{2^1\Pi}$, $1^3\Delta$, $3^3\Sigma^-$ and $1^3\Sigma^-$; and channel c $\underline{3^1\Sigma^+}$, $3^{3,1}\Pi$ and $1^3\Sigma^+$. Underlined are the (attractive) states which can interact with (repulsive) states of the same symmetry generated by channels I to III. Thus, only five repulsive states of types I, II, and III, from a total of six, have attractive counterparts in channels a, b, and c. The exception corresponds to $2^1\Sigma^+$, a strongly repulsive potential in all cases (see below). Similar arguments were presented recently[3c,20c] for ClH^{2+} and BrH^{2+}, where the reported potential curves reproduce well the literature data (IPs, R_e's, ω_e's, Franck−Condon factors, tunneling lifetimes). The semiempirical procedure used in both studies[3c,20c] combines together, and substantially improves, semiquantitative arguments previously advanced in the literature about the stability of dications.[6−8,32] It should be noted, however, that most of the properties studied here (fine and hyperfine structure, nuclear quadrupole couplings, etc.) lie beyond the capabilities of the semiempirical approach applied to ClH^{2+}/BrH^{2+}.[3c,20c]

We first consider $\Delta E_d(R)$, which is negative throughout (Table 2), i.e., all states destabilize relative to $(X^+ + H^+)$. For a metastable potential, $\Delta E_d(R)$ can be identified with (i) the dissociation energy, $D_e = \Delta E_d(R_e)$, for the minimum at $R = R_e$, and (ii) the kinetic energy release, KER $= |\Delta E_d(R_b)|$, for the maximum at the barrier geometry $R = R_b$. On the other hand, for a repulsive potential, $|\Delta E_d(R)|$ is the KER value detectable via $XH \rightarrow XH^{2+}$ ionization if the parent neutral geometry $R = R_e(XH)$ is chosen. As expected, the absolute value $|\Delta E_d(R)|$ decreases along the series, from about 9.0−11.3 eV in FH^{2+}, to 4.3−7.3 eV in ClH^{2+}, and to 3.0−6.5 eV in BrH^{2+}. At short R, the repulsive $2^1\Sigma^+(\pi^4)$ potential retains its asymptotic structure $X^+(^1S)+H^+$, and accordingly $\Delta E_d(R) \approx -1/R$ in all XH^{2+} ions (see Figure 2 in ref 16b for the $2^1\Sigma^+$ potential versus $1/R$ in ClH^{2+}).

$\Delta E_{el}(R)$ is always positive (all states lie below the repulsive potential $1/R$). Such stabilization relates to the shift of electron density into the internuclear region due to the mixing between repulsive $(X^+ + H^+)$ and attractive $(X^{2+} + H)$ structures. For a metastable state, the larger $\Delta E_{el}(R_e)$ the deeper the potential well. As discussed in several papers on multiply charged AB^{n+} ions (Be_2^{2+}, B_2^{2+}, BN^{2+}, Al_2^{3+}, and BN^{3+}),[32] the $\Delta E_{el}(R)$ function associated with a metastable state looks like a regular bound potential curve,[32] and the same applies to present XH^{2+}'s (as shown for FH^{2+} and ClH^{2+} in ref 33).

Metastable $X^3\Sigma^-$, $1^1\Delta$ have similar ΔE_{el}'s, on average 5.6 eV in ClH^{2+} and 6.2 eV in BrH^{2+}. The third metastable state $(1^1\Sigma^+)$ has in each case a $\Delta E_{el} \approx 1.3$ eV smaller. Next, one finds $1^{3,1}\Pi$ with an average $\Delta E_{el} \approx 2.7$ eV. Finally, $\Delta E_{el}(2^1\Sigma^+) \approx 0$ throughout, i.e., $2^1\Sigma^+$ is repulsive at all R's (channels a−c generate only one structure $(X^{2+} + H^+)$, which preferentially stabilizes the $1^1\Sigma^+$ potential instead).

Taking into account electronic configurations, the degree of stabilization in ClH^{2+}/BrH^{2+} ranges from strong for $1\sigma^2 2\sigma^2\pi^2$ (metastable: $X^3\Sigma^-, 1^1\Delta, 1^1\Sigma^+$) to medium for $1\sigma^2 2\sigma\pi^3$ (moderately repulsive: $1^{3,1}\Pi$) to rather weak for $1\sigma^2\pi^4$ (strongly repulsive: $2^1\Sigma^+$). Thus, maximal occupation of the 2σ MO leads to metastability, whereas $2\sigma^0$ results in a repulsive state; that is, this MO is of bonding character. As X^+ and H^+ come closer together, and assuming 2σ is occupied, such $np_\sigma(X)/1s(H)$ mixing allows for some charge density on X^+ to be transferred to H^+; that is, $E(R)$ is less repulsive than $1/R$, or even locally bound (metastability). Regarding double-ionization from XH $[X^1\Sigma^+(2\sigma^2\pi^4)]$, metastable XH^{2+} states are thus selectively generated upon extraction of two nonbonding π electrons.

TABLE 3: Equilibrium Data (MRDCI) for the Bound $1^5\Sigma^-$ States of XH^{2+} (X = F, Cl, and Br), Including Magnetic and Electric Hyperfine Parameters

$1^5\Sigma^-(\sigma\pi^2\sigma^*)$	$^{19}FH^{2+}$	$^{35}ClH^{2+}$ [a]	$^{79}BrH^{2+}$ [b]
R_e (bohr)	4.34	5.50	5.91
ω_e (cm^{-1})	670	390	410
D_e (cm^{-1})[c]	3850	1290	1150
T_e (eV)	(11.9)	5.7	4.9
ΔE_I (eV)[d]	20.9	10.0	7.9
ΔE_{II} (eV)[e]	57.8	41.1	37.1
ΔE_{III}(eV)[f]	47.5	31.6	≈27.7
X center			
A_{iso}(MHz)	50(100)	35(10)	15(100)
A_{dip}(MHz)	4.0(25)	0.4(1)	1.2(5)
q (au)	0.05(3)	0.06(1)	0.08(1)
H center			
A_{iso}(MHz)	308(10)	316(5)	320(10)
A_{dip}(MHz)	6.6(2)	3.3(1)	2.4(2)
q (au)	−0.022(2)	−0.012(1)	−0.010(1)

[a] MRDCI: $R_e = 4.93$ bohr; $\omega_e = 772$ cm^{-1}, and $D_e = 2100$ cm^{-1}.[12,14] [b] MRDCI: weakly bound, by less than 500 cm^{-1}.[13,15] [c] Dissociation energy into $X^{2+}(^4S)+H(^2S)$, using $E(1^5\Sigma^-)$ at $R = 500$ bohr. [d] Relative to $X^+(^3P) + H^+$, based on atomic data,[9] and present D_e's. [e] Ad. IP($\pi^2 \rightarrow \infty$) relative to XH ($X^1\Sigma^+$, $v = 0$), based on atomic data[9] and D_0(XH).[30] [f] Ad. IP($\pi^2 \rightarrow \infty$) relative to $(B,V)^1\Sigma^+$ ion-pair state in XH.[30]

Recently, Huang and Zhu[33] have described XH^{2+} (X = halogen) and ClH^{3+} potential curves via a general expression of type $V(R) = V_{Coul}(R) - |V_{MS}(R)|$, which obviously coincides with ours written in a slightly different terminology, $\Delta E_d(R) = V_{Coul}(R) - \Delta E_{el}(R)$. They calculated the $V(R)[\Delta E_d(R)]$ potential at the single-reference, double-excitation CI (CID) level, using triple-ζ polarization basis sets for F/Cl and effective core potentials/smaller bases (LanL1dz) for Br/I. The term $V_{MS}(R)$ $[-\Delta E_{el}R]$ was represented by the (Murrel-Sorbie) analytical term $V_{MS}(R) = -[D_0\ (1 + a_1\rho + a_2\rho^{\ 2} + a_3\rho^3)]\ \exp(-a_1\rho)$, where ρ stands for $\rho(R) = (R - r_0)$; the constants D_0, a_i, and r_0 were fitted to the CID potentials. Using the reported data,[33] we calculate $-\Delta E_d(R)$ and $\Delta E_{el}(R)$ for the $X^3\Sigma^-$ potentials of XH^{2+} (also for $1^4\Sigma^-$ of ClH^{3+}, see 3.1.4) at the geometries used here. As seen in Table 2, the single-reference CID potentials are more repulsive than those at the multireference level (our $-\Delta E_d/\Delta E_{el}$ values are smaller/larger, by up to ≈0.9 eV, due to a more flexible description of repulsive-attractive mixings).

3.1.3. Bound $1^5\Sigma^-$ State. Tables 1 and 3 list data on $1^5\Sigma^-$, whereas Figure 2 shows corresponding potential curves. As guidance for future experimental characterization of $1^5\Sigma^-$, Table 3 lists (besides T_e) some other energy differences relative to $E(1^5\Sigma^-)$ at its R_e minimum, namely, (i) ΔE_I relative to $E[X^+(^3P)+H^+]$, the lowest dissociation channel of XH^{2+}, (ii) ΔE_{II} relative to the GS of neutral XH (i.e., adiabatic IP[$XH(X^1\Sigma^+,\sigma^2\pi^4) \rightarrow XH^{2+}(1^5\Sigma^-,\sigma\pi^2\sigma^*)+2e^-$], a triple-excitation process), and (iii) ΔE_{III} relative to the long-range minimum[30,31] of the ion-pair excited state $^1\Sigma^+(\sigma\pi^4\sigma^*)$ in XH (i.e., adiabatic IP[$XH(^1\Sigma^+,\sigma\pi^4\sigma^*) \rightarrow XH^{2+}(1^5\Sigma^-,\sigma\pi^2\sigma^*)+2e^-$], a double-excitation process).

We find, for the first time, that this quintet state is bound in FH^{2+}, like in ClH^{2+}/BrH^{2+},[12−15] a rather peculiar situation since all other FH^{2+} potentials are repulsive. (By contrast, $1^5\Sigma^-$ is repulsive in NH, PH, OH^+, and SH^+,[31a] radicals isovalent with present XH^{2+}.) $1^5\Sigma^-$ correlates with channel a $[X^{2+}(^4S)+H(^2S)]$, which also gives rise to $2^3\Sigma^-$ (moderately repulsive in ClH^{2+}).[12,14] Both Σ^- states are described by the configuration $\sigma\pi^2\sigma^*$, which can be formally partitioned into $\sigma\pi^2[X^{2+}(^4S)]$ plus $\sigma^*[H(^2S)]$. Such a structure (two S states weakly interacting with each other) is reflected in the hfs of $1^5\Sigma^-$ (Table 3): A_{iso}, A_{dip}, and q values are all small (cf with atomic or molecular

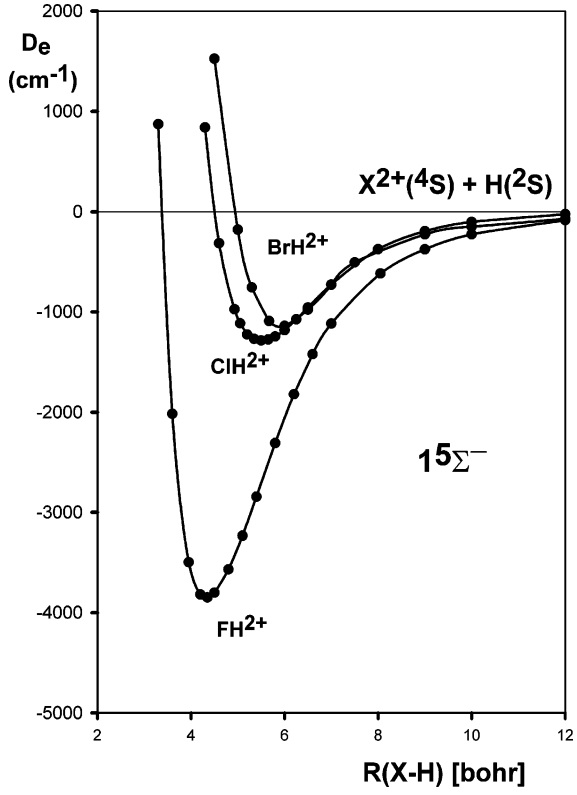

Figure 2. Potential curve of the bound $1^5\Sigma^-(\sigma\pi^2\sigma^*)$ state in FH^{2+}, ClH^{2+}, and BrH^{2+} (MRDCI data, correlating 6, 12, and 22 electrons, respectively).

data for s^2p^5, s^2p^4, or $\sigma^2\pi^2$ states, sections 3.2 and 3.3), except for A_{iso}(H) having a common value of ca. 315 MHz in the three ions. This represents about 22% *s*(H) character, i.e., slightly below 25% for a normalized SDD.

Relative to $X^3\Sigma^-$ (Tables 1 and 3), $1^5\Sigma^-$ lies very high in FH^{2+} but much lower in the other ions, about 17 vs 9 eV, vertical, or about 12 vs 5.3 eV, adiabatic. The vertical IP[XH-$(X^1\Sigma^+) \rightarrow XH^{2+}(1^5\Sigma^-)$] is calculated (in eV) to be 70.5 for FH, 46.5 for ClH, and 42.1 for BrH, which also represent energy thresholds for generating (X^{2+}+H) products (see 3.1.4).

The $1^5\Sigma^-$ potential is relatively well bound in FH^{2+} ($D_e \approx 3900$ cm^{-1}, $\omega_e = 670$ cm^{-1}) but much less so in the other dications (on average, $D_e \approx 1220$ cm^{-1}, $\omega_e \approx 400$ cm^{-1}). According to the R_e data for $X^1\Sigma^+$(XH) and $1^5\Sigma^-(XH^{2+})$ from Tables 1 and 3, their potential minima differ from about 2.6 to 3.3 bohr for the three systems; that is, there is little chance for detecting the $1^5\Sigma^-$ minima via ionization from the GS of XH, due to extremely unfavorable Franck−Condon factors. As well, the triple-excitation character of the process $X^1\Sigma^+ \rightarrow 1^5\Sigma^-$ (+2e$^-$) would be of very low efficiency. In short, experimental detection of $1^5\Sigma^-$ via (vertical or adiabatic) double-ionization from $X^1\Sigma^+$(XH) seems quite unlikely.

There exists, in principle, a more favorable mechanism for generating $1^5\Sigma^-$ via ionization from another neutral $^1\Sigma^+$(XH) state, namely the (ion-pair) excited-state known from emission studies as $B(2)^1\Sigma^+$ in FH/ClH, and as $V^1\Sigma^+$ in BrH.[30,31] According to the literature,[30,31] all neutral $X^1\Sigma^+(\sigma^2\pi^4)$ GSs are highly ionic (X^-H^+) at equilibrium. Along the path toward $X(^2P)+H(^2S)$ products, however, the contribution to the GS of $\sigma^2\pi^4$ [X^-H^+, attractive] decreases whereas that of $\sigma\pi^4\sigma^*$[X^0H°, repulsive] increases. An avoided crossing between these diabatic potentials results in strongly ionic $^1\Sigma^+$ excited states with R_e's of 3.95, 4.75, and 5.1 bohr for FH, ClH, and BrH, respectively,[30,31] which are shorter than $R_e(1^5\Sigma^-)$ by 0.4 bohr in FH^{2+} and 0.7 bohr in ClH^{2+}/BrH^{2+}. Thus, due to more favorable Franck−Condon factors, the existence of $1^5\Sigma^-(XH^{2+})$ could be proved via double ionization from the ion-pair $(2)^1\Sigma^+$ state of XH. The ΔE_{III} data (Table 3) show that such IPs require ≈10 eV less energy than from the GSs. Double-ionization $\pi^2 \rightarrow \infty$ operating in both processes $\sigma^2\pi^4(X^1\Sigma^+) \rightarrow \sigma^2\pi^2(X^3\Sigma^-)$ and $\sigma\pi^4\sigma^*(^1\Sigma^+) \rightarrow \sigma\pi^2\sigma^*(^5\Sigma^-)$ should take place with comparable ionization cross-sections.[1,6]

3.1.4. Stability of Triply Ionized XH^{3+} Ions. Table 4 lists the single, double, and triple IPs from $X^1\Sigma^+(\sigma^2\pi^4)$ of XH at R_e(expt.)[30] into the ionic states: (I) $X^2\Pi(\pi \rightarrow \infty)$ of XH^+, (II) $X^3\Sigma^-(\pi^2 \rightarrow \infty)$ and $1^5\Sigma^-(\pi^2 \rightarrow \infty, \sigma \rightarrow \sigma^*)$ of XH^{2+}, and (III) $1^2\Pi(\pi^3 \rightarrow \infty)$ and $1^4\Sigma^-(\sigma\pi^2 \rightarrow \infty)$ of XH^{3+}. Also included are the stability parameters $\Delta E_d(R_e) = [E(\infty) - E(R_e)]$ and $\Delta E_{el}(R_e) = [2/R + \Delta E_d(R_e)]$ for the trications.

As seen in Table 4, corresponding IPs in the ClH/BrH series are not too different from each other (about 1 eV for XH^+ to 7 eV for XH^{3+}), whereas the differences between FH and ClH are much larger (3.5−30 eV). Vertical IP($\pi^2 \rightarrow \infty$)'s into $X^3\Sigma^-(XH^{2+})$ of 47.50, 35.02, and 32.08 eV for FH, ClH, and BrH, respectively, are in good agreement with experimental values of 35.9 ± 0.2/35.59 eV for ClH and 32.4 ± 0.4/32.9 eV for BrH. For each family of hydrides, it approximately holds that the double (II) and triple (III) IPs are about three and six times the value of the single IP (I), respectively.[1a] Since $IP(XH^{3+}) \approx 2\ IP(XH^{2+})$, an experimental[6] $IP(IH^{2+}) = 30.0 \pm 0.5$ eV for iodine hydride would suggest $IP(IH^{3+}) \approx 60$ eV (unknown), which, as expected, lies somewhat below $IP(BrH^{3+}) = 65.44$ eV (Table 4).

We have studied for XH^{3+} the states $1^4\Sigma^-(\sigma\pi^2)$ and $1^2\Pi(\sigma^2\pi^1)$, which respectively correlate with $^4S < {}^2D$ of X^{2+}, plus H^+. At R_e(XH), their relative ordering is $1^4\Sigma^- < 1^2\Pi$ in FH^{3+}, $1^4\Sigma^- \approx 1^2\Pi$ in ClH^{3+}, and $1^4\Sigma^- > 1^2\Pi$ in BrH^{3+} (Table 4). All trication states are expected to be repulsive. At the R_e's considered (Table 4), the repulsive potentials $V_{Coul} = (q^{2+})(q^+)/R_e = 2/R_e$ are 31.4, 22.6, and 20.5 eV for the F, Cl, and Br series, respectively. The $|\Delta E_d|$ values are always smaller, indicating that both $1^4\Sigma^-$, $1^2\Pi$ lie below the corresponding *V* values listed above. Like for XH^{2+} ions, some electronic charge density is thus transferred from X^{2+} into the bonding region (toward H^+). $\Delta E_{el}(R)$ gives a more quantitative picture: between FH^{3+} and BrH^{3+}, it ranges from 4.8 to 7.4 eV for $1^2\Pi(\sigma^2\sigma^2\pi^1)$ and from 3.3 to 4.6 eV for $1^4\Sigma^-(\sigma^2\sigma\pi^2)$. A larger stabilization in $1^2\Pi$ relates to this state having one extra σ-electron: the charge distribution $\sigma^2\sigma^2\pi^1$ is more effective for screening nuclear repulsion than $\sigma^2\sigma\pi^2$.

Two calculations[11a,e] on FH^{3+} place $1^2\Pi$ slightly above 100 eV, close to our result of 102.67 eV (Table 4). Both studies, however, overlooked the $1^4\Sigma^-$ state, which is ≈2.7 eV more stable at R_e(XH). Theoretical results are available on ClH^{3+} [33] but apparently not on BrH^{3+}. The experimental energy threshold for formation of (X^{2+}+H) products has been reported for ClH[18h] and BrH,[19c] whereas that for generating (X^{2+}+H^+) is known for ClH only.[18h] We are unaware of similar information for FH. The first process is assumed to take place via $1^5\Sigma^-$ of XH^{2+} dissociating into $X^{2+}(^4S) + H(^2S)$, whereas the second one involves $1^2\Pi$ of ClH^{3+} correlating with $X^{2+}(^2D) + H^+$. Our IP($1^5\Sigma^-$, XH^{2+})'s of 46.5 and 42.0 eV for ClH^{2+} and BrH^{2+}, respectively, are in good agreement with experimental energy thresholds for Cl^{2+}/Br^{2+} formation, 46.8 ± 1.5 and 40.2 ± 0.4 eV (a recent value of 42.8 ± 1.1 eV[18i] for Cl^{2+} formation via $1^5\Sigma^-(ClH^{2+})$ is not supported by our results). Also, IP(ClH^{3+})'s calculated at 72.25 eV ($1^2\Pi$) and 72.72 eV ($1^4\Sigma^-$) nicely agree with 72 ± 2 eV, expt.[18h] Although both ClH^{3+} states could have

TABLE 4: Vertical (Single, Double, and Triple) Ionization Potentials IP (eV) of XH, and Relative Energies $\Delta E_d(R)$ and $\Delta E_{el}(R)$ for XH^{3+} Trications (MRDCI Data)[a]

			FH		ClH		BrH	
			tw	lit.[b]	tw	lit.[b]	tw	lit.[b]
			IP		IP		IP	
XH	$X^1\Sigma^+$	$(\sigma^2\pi^4)$	0.00		0.00		0.00	
XH^+	$X^2\Pi$	$(\sigma^2\pi^3)$	15.91	16.06[c]	12.44	12.74[c]	11.53	11.67[c]
XH^{2+}	$X^3\Sigma^-$	$(\sigma^2\pi^2)$	47.50		35.02	35.59[d]	32.08	32.4(4)[e]
XH^{2+}	$1^5\Sigma^-$	$(\sigma\pi^2\sigma^*)$	70.50		46.50	46.8(15)[f]	42.00	40.2(4)[e]
XH^{3+}	$1^2\Pi$	$(\sigma^2\pi^1)$	102.67	100.35[g]	*72.25*[h]	72(2)[f]	*65.44*[h]	
XH^{3+}	$1^4\Sigma^-$	$(\sigma\pi^2)$	*100.00*[h]		72.72		66.25	
			$-\Delta E_d(R_e)$	$\Delta E_{el}(R_e)$	$-\Delta E_d(R_e)$	$\Delta E_{el}(R_e)$	$-\Delta E_d(R_e)$	$\Delta E_{el}(R_e)$
XH^{3+}	$1^2\Pi$	$(\sigma^2\pi^1)$	26.6	4.8	15.6	7.0	13.1	7.4
XH^{3+}	$1^4\Sigma^-$	$(\sigma\pi^2)$	28.1	3.3	18.3	4.3	15.8	4.7
					(19.3)[i]	(3.2)[i]		

[a] Calculations at R_e (bohr) of 1.7329 (FH), 2.41 (ClH), and 2.66 bohr (BrH), expt.[30] Number of electrons correlated, from XH^{3+} to XH: 5−8 (FH), 11−14 (ClH), and 21−24 (BrH). $X^1\Sigma^+$ energy (au): −100.1914, −460.3297, and −2573.3595 (left to right). $\Delta E_d(R_e) = [E(\infty) - E(R_e)]$, and $\Delta E_{el}(R_e) = [2/R + \Delta E_d(R_e)]$, where $E(\infty)$ is $E[X^{2+}(^4S)+H^+]$ for $1^4\Sigma^-$, and $E[X^{2+}(^2D)+H^+]$ for $1^2\Pi$ of XH^{3+}. [b] Selected experimental results (except for FH^{3+}, footnote g). [c] Reference 30. [d] Reference 18e. Others: 35.9;[12] and 35.4(6).[18i] [e] Reference 19c. Others ($^3\Sigma^-$): 32.9,[19b] 32.67($^3\Sigma_0^-$),[3c] and 32.61.[19d] [f] Reference 18h. An expt.[18i] threshold for Cl^{2+} formation of 42.8(±1.1) eV not supported by our data. [g] ΔSCF data;[11a] IP(XH^{3+}, $1^2\Pi$)= 102.8 eV, calculated using $\Delta E[1^2\Pi\text{-}X^3\Sigma^-]$= 55.3 eV (MRDCI)[11e] and our calculated IP(XH^{2+}, $X^3\Sigma^-$). [h] Ground state. [i] Values at $R = 2.41$ bohr calculated here using V(R) potential (CID level) from ref 33.

TABLE 5: Reference Calculations on the Magnetic and Quadrupolar Parameters of X and X^+ Atomic Species

X/X^+		$\lvert\varphi(0)\rvert^2$ (au)	A_{iso} (MHz)	$\langle r^{-3}\rangle_d$ (au)	A_{dip} (MHz)	$\langle r^{-3}\rangle_q$ (au)	q (au)	$\lvert eQq\rvert$ (MHz)
^{19}F atom (^2P)								
(MP)[2s2p]	34	[12.53]	[52870]	[8.766]	[1760]			
(FZP)[2s2p]	35	[11.36]	[47935]	[8.126]	[1632]			
	36b	0.0470	198	7.963	1599	6.880	2.752	
	36c	0.0496	209	7.950	1596	6.852	2.741	
	36d	0.0692	275	7.935	1593	6.867	2.747	
	36e			8.019	1610	6.907	2.763	
	tw	0.065(40)	275(170)	7.97(25)	1600(50)	7.13(25)	2.85(10)	
expt.	36a	0.0717	302	8.14	1634			
$^{19}F^+(^3P)$	tw	0.047(36)	200(150)	9.09(25)	1825(50)	8.35(25)	3.34(10)	
^{35}Cl atom (^2P)								
(MP)[3s3p]	34	[12.81]	[5723]	[8.389]	[176]			
(FZP)[3s3p]	35	[10.46]	[4673]	[7.884]	[165]			
	37c	0.034	15.2					
	tw	0.035(20)	16(9)	7.26(5)	122(1)	6.80(50)	2.72(20)	52(4)
expt.	37d	0.079(4)	35.3(18)	7.917(23)	165.7(5)	7.15[a]	2.86[a]	55
$^{35}Cl^+(^3P)$	tw	0.15(1)	67(5)	8.12(5)	136(1)	7.95(25)	3.18(10)	61(2)
^{79}Br atom (^3P)								
(MP)[4s4p]	34	[24.47]	[27480]	[15.25]	[818]			
	37c	−0.053	−60					
	tw	−0.26(1)	−292(11)	12.82(28)	620	12.51(25)	5.01(10)	368(7)
expt.	38c	(0.135)[b]	(1320)[b]	14.18	686[c]	13.09[a]	5.24[a]	385
$^{79}Br^+(^3P)$	tw	−0.428(125)	−480(140)	14.46(28)	698(14)	14.31(25)	5.73(10)	421(7)

[a] References 28 and 39. [b] Weltner[34,38d] reports these isotropic data from gas-phase studies.[37b,38c] A_{iso}(matrix)= 1433 MHz. [c] A_{dip}= −148 MHz (gas) and −505 MHz (matrix).[34,38d]

been generated in the ionization chamber, predissociation interactions will result in the formation of $[Cl^{2+}(^4S)+H^+]$ products exclusively (since $1^2\Pi$ is crossed by $1^4\Sigma^-$ at large R). As seen by the $\Delta E_d/\Delta E_{el}$ data (Table 4), the CID potential[33] for $1^4\Sigma^-(ClH^{3+})$ seems to be too steep, like as for XH^{2+} ions (3.1.2).

3.2. Magnetic Hyperfine Coupling Constants: A_{iso} and A_{dip}. *3.2.1. Atomic States.* We analyze the quality of our results by reporting in Table 5 the hfs parameters for the $^2P(X)$ and $^3P(X^+)$ atomic states.[34−39] They are (i) in atomic units, the *s*-spin-density $\varphi^2(0)$, the expectation values $\langle r^{-3}\rangle_d$ and $\langle r^{-3}\rangle_q$ evaluated with SDD and CDD, respectively, and the electric field gradient (efg) parameter $q = (2/5)\langle r^{-3}\rangle_q$ and (ii) in MHz, the magnetic terms $A_{sio} = (8\pi/3)K\varphi^2(0)$ and $A_{dip} = (2/5)K\langle r^{-3}\rangle_d$ (with $K = g_e g_n \beta_e \beta_n$)[34] and the electric quadrupole parameter $(eQ)q$ (please note that $Q = 0$ for ^{19}F). Neither experimental nor theoretical hfs data are currently available for F^+, Cl^+, or Br^+, to the best of our knowledge. Experimental hfs are known for all three neutral atoms.[36−39] Regarding theoretical data, F is the only atom for which all its hfs parameters have been studied,[36] whereas solely $\varphi^2(0)$ and A_{iso} have been calculated for Cl and Br.[37,38]

$A_{dip}(X^+)$ should be larger than $A_{dip}(X)$, and also $q(X^+) > q(X)$, since $\langle r^{-3}\rangle$ increases[39,40] as the electronic cloud becomes more compact upon ionization $X \rightarrow X^+$. Although hfs's have not been measured for these X^+ ions to confirm such a trend, it is indirectly supported experimentally by the fact that $\zeta(X^+) > \zeta(X)$, where the atomic spin−orbit coupling constant ζ is proportional to $\langle r^{-3}\rangle$.[41] Finally, the isotropic term $A_{iso}(X^{n+}) \propto \varphi^2(0)$ is expected to increase with n as well.

Atomic reference data[34,35] of magnetic hf parameters for *ns* and *np* orbitals in neutral X are also given in Table 5. (Our $\langle r^{-3}\rangle_d$ and A_{dip} correspond to $\langle r^{-3}\rangle$ and $(2/5)P$ in ref 34.) The standard Morton and Preston (MP)[34] values are systematically

TABLE 6: Hyperfine Coupling Constants A_{iso}/A_{dip} and $A_{||}/A_{\perp}$ (in MHz) Calculated for XH^{2+} ($X^3\Sigma^-$), and Comparison with Similar Data for XH^+ ($X^2\Pi$) Ions (X Isotopes ^{19}F, ^{35}Cl, and ^{79}Br)

		X atom				^1H[a]	
state	ref	A_{iso} (b_F)	A_{dip} ($c/3$)	$A_{||}$ ($b+c$)	$A_{\perp}$ (b)	A_{iso} (b_F)	A_{dip} ($c/3$)
$X^3\Sigma^-(\sigma^2\pi^2)$ state							
FH^{2+}	tw	230(50)	−900(5)	−1570(60)	1130(55)	−36(2)	37(1)
ClH^{2+}	tw	110(15)	−86(1)	−62(17)	196(16)	−54(2)	13(1)
expt. $^{35}ClD^{2+}$	4	167(25)	(positive)[b]			[−52][c]	
expt. $^{35}ClD^{2+}$	3	162(30)	[−30(25)][d]	[−102(70)][e]	[192(55)][e]		
BrH^{2+}	tw	300(50)	−400(5)	−500(60)	700(55)	−57(3)	10(1)
$X^2\Pi(\sigma^2\pi^3)$ state[f]							
FH^+	28	630(5)	−810(5)	−990(15)	1440(10)	−79(4)	52(1)
	theor.	575	−832	−1089	1407	−69	61
	expt.	549(96)	−769(31)	−988(158)	1317(127)		
ClH^+	28	85(15)	−81(2)	−77(19)	166(17)	−64(2)	14(1)
	expt.				132(46)		
BrH^+	28	300(30)	−374(2)	−448(34)	674(32)	−67(2)	9(1)
	expt.	155(108)	−470(28)	−784(5)	625(82)		

[a] $A_{||}/A_{\perp}$ (MHz), tw: 38(4)/−73(3) for FH^{2+}; −28(4)/−67(3) for ClH^{2+}; and −37(5)/−67(4) for BrH^{2+}. See ref 28 for corresponding XH^+ data. [b] Scaled LSF data ranging from −4 to +204 MHz. [c] Estimated here using $b_F(^2H) = -16$ MHz calculated at the UQCISD level.[2] [d] Estimated[2] using $c/3 = -75(21)$ MHz for $^{37}ClD^{2+}$. [e] Calculated here with given b_F and c data. [f] See ref 28 for theoretical and experimental references.

too large, as noted by Fitzpatrick et al. (FZP).[35] We also found that the conversion factor from $\varphi^2(0)$ [au] to A_{iso} [MHz] used in ref 34 for ^{79}Br is incorrect, i.e., $\varphi^2(0) = 24.47$ au corresponds to $A_{iso}(^{79}Br) = 27\,480$ MHz rather than to 32 070 MHz.[34]

All experimental data agree in that $\langle r^{-3}\rangle_d$ is larger than $\langle r^{-3}\rangle_q$, by about 10%. Regarding the isotropic contribution, the experimental $A_{iso}(^2P, s^2p^5)$'s are up to 2 orders of magnitude smaller than the reference parameters for *ns* orbitals, making the calculation of accurate A_{iso}'s difficult.[42] The $s(X/X^+)$ densities lie below 1% and should be similarly low on X of XH^{2+}; that is, not too much can be learned about bonding from $A_{iso}(X)$, in contrast to the key role played by $A_{iso}(H)$. Similarly, $A_{dip}(X)$ and $q(X)$ give a realistic picture about bonding. Since the structure $(X^{2+}+H)$ is stabilizing, a trend between molecular and atomic data can be established for a given hfs parameter (p^X) on atom X, namely $p^X(XH^{2+}) \gtrsim p^X(X^+) > p^X(X)$. Here, p^X stands for the magnetic [$A_{dip}(X)$] or quadrupole electric [$eQq(X)$] coupling constant (if p^X is negative, this relationship applies to its absolute values).

3.2.2. Molecular Dicationic States. A_{iso}, A_{dip}, $A_{||}$, and $A_{\perp}$ (or b, b_F, and c)[34,43,44] for $X^3\Sigma^-(XH^{2+})$ are listed in Table 6, along with data for XH^+ ions (studied by us using similar methods).[28] Note the equivalencies $A_{iso} = b_F = (b + c/3)$; $A_{dip} = c/3$; $A_{||} = (A_{iso} + 2A_{dip}) = (b + c)$; and $A_{\perp} = (A_{iso} - A_{dip}) = b$.[34]

The halogen $A_{iso}(X)$'s lie below 700 cm^{-1}, quite small compared with "atomic" $s(X)$ values from 5000 to 50 000 MHz (Table 5). $A_{dip}(X)$ is negative in $X^2\Pi(\sigma^2\pi^3)$ of XH^+ and $X^3\Sigma^-(\sigma^2\pi^2)$ of XH^{2+}, in line with π-SOMOs having their SDD maximum perpendicular to the bond. Due to the small $A_{iso}(X)$'s but large (and negative) $A_{dip}(X)$'s, the ESR spectra of these XH^{2+}'s should be quite anisotropic, as manifested by the opposite signs of $A_{||}(X)$ and $A_{\perp}(X)$ constants (Table 6).

The H spin-density is small for both XH^+ and XH^{2+} since the π-type SDDs are mainly localized on X. Relevant is the fact, however, that the H hfccs in XH^{2+} are different from zero and, therefore, proving the transfer from halogen SD to the "proton". Taking $A_{iso}(1s, H) = 1420$ MHz as reference,[34] the average hydrogenic contributions are not higher than 6%. Please note that negative $A_{iso}(H)$'s are characteristic for XH's with $\sigma^2\pi^m$ GSs, as found experimentally[34,43] for $X^2\Pi$ radicals [CH ($m = 1$), OH ($m = 3$)] and $X^3\Sigma^-$ ($m = 2$) systems [NH, OH^+].

Figure 3 displays the variation with R of the magnetic hfccs of $^{35}ClH^{2+}$. Clearly, $A_{dip}(Cl)$ differs little from asymptotic $Cl^+(^3P)$, whereas $A_{iso}(Cl)$ increases slightly at short R. Further,

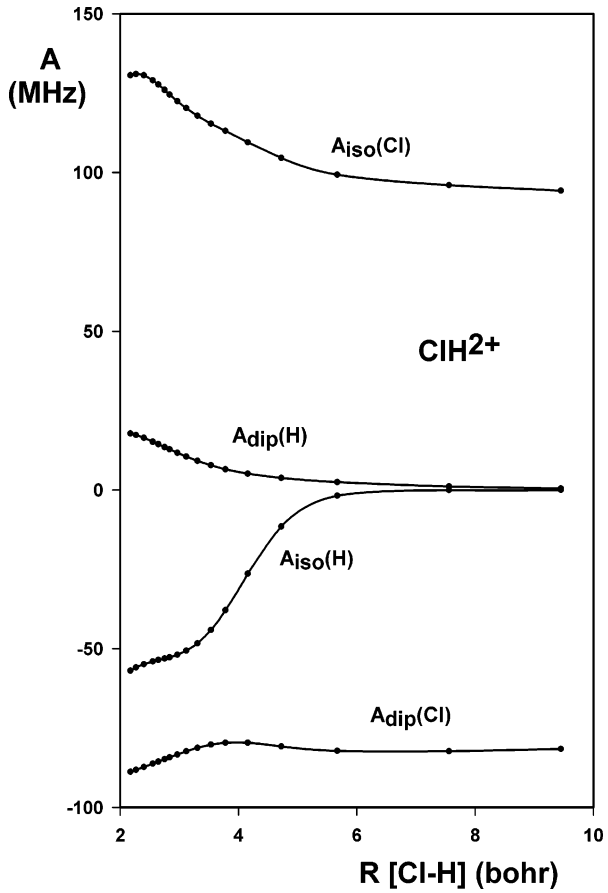

Figure 3. A_{iso} and A_{dip} values for the $X^3\Sigma^-$ state of $^{35}Cl^1H^{2+}$ as a function of bond length (QCISD/cc-pVTZ data, correlating 6 electrons).

$A_{iso}(H)$ changes gradually from a zero value at $R = \infty$ to −54 MHz (about 4%1s(H)) at R_e ($X^3\Sigma^-$). The small $A_{dip}(H)$ arises from the proton being placed in a strongly anisotropic spin-density region due to Cl^+ (in general, $A_{dip}(H) \approx 0$ in all diatomic hydride radicals reported in the literature).[34,43]

3.3. Quadrupole Hyperfine Coupling Constants: *eQq* (*q* = Electric Field Gradient). Experimental and theoretical efg and nqcc data (q and eQq, respectively) are available for XH ($X^1\Sigma^+$) and XH^+ ($X^2\Pi$, $A^2\Sigma^+$)[28] but not for XH^{2+} ($X^3\Sigma^-$) dications (X = F, Cl, and Br). Magnetic hfccs allow us to investigate structural changes between XH^+ and XH^{2+}, whereas

TABLE 7: Electric Field Gradient (*q*) and Nuclear Coupling Constant (*eQq*) Calculated for the XH, XH^+, and XH^{2+} Systems (X = ^{19}F, ^{35}Cl, and ^{79}Br)[a]

state[b,c]		*q*(X) (au)	*eQq*(X) (MHz)	*q*(H/D) (au)	*eQq* (D) (kHz)
FH	$X^1\Sigma^+$	2.67(5)		0.56(2)	376(13)
FH^+	$X^2\Pi$	0.18(10		0.258(4)	170(2)
		8.98(4)		0.065(1)	43(1)
	$A^2\Sigma^+$	7.40(15)		0.105(5)	69(3)
FH^{2+}	$X^3\Sigma^-$	4.90(10)		0.098(2)	66(1)
ClH	$X^1\Sigma^+$	3.30(5)	−63.3(9)	0.292(5)	196(3)
ClH^+	$X^2\Pi$	0.65(2)	−12.5(4)	0.210(1)	138(1)
		8.83(3)	−169(1)	−0.038(1)	−25(1)
	$A^2\Sigma^+$	8.50(20)	−163(4)	0.107	70(10
ClH^{2+}	$X^3\Sigma^-$	3.08(10)	−59(2)	0.071	46(2)
BrH	$X^1\Sigma^+$	7.0(1)	514.8(74)	0.230(5)	155(3)
BrH^+	$X^2\Pi$	2.00(15)	147(3)	0.175(2)	115(1)
		16.8(3)	1236(22)	0.029(1)	19(1)
	$A^2\Sigma^+$	17.0(50)	1250(40)	0.082(2)	54(1)
BrH^{2+}	$X^3\Sigma^-$	5.0(2)	367.7(127)	0.080(10)	53(1)

[a] Nuclear spin, $I = 3/2$ for Cl and Br, and $I = 1$ for D(^{2}H), with corresponding conversion factors *q* (au) to *eQq* (MHz): 19.1818, 73.5429, and 0.6579.[28] The isotopes ^{1}H and ^{19}F have $Q = 0$. [b] First entry (all states): $q_0 \equiv q_{zz} = \partial^2V/\partial^2z$. Second ($X^2\Pi$): $q_2 \equiv (q_{xx} - q_{yy}) = \partial^2V/\partial^2x - \partial^2V/\partial^2y$. [c] See ref 28 for detailed comparisons and literature references for XH/XH^+ states.

q's and nqcc's are defined for the whole series XH → XH^+ → XH^{2+} (except for X = ^{19}F with nuclear quadrupole $Q = 0$).

Table 7 lists the median values calculated for the efg parameter q_i ($i = 0$ and 2) and corresponding nqcc's. Throughout, the first entry corresponds to the parallel component q_0 [$\equiv q_{zz}$] = ∂^2V/∂^2z. For $X^2\Pi$ states, a second (perpendicular) component is needed, q_2 [$\equiv(q_{xx} - q_{yy})$] = $\partial^2V/\partial^2x - \partial^2V/\partial^2y$].[28,44] The same distinction applies to eQq_i. The nqcc component eQq_i (MHz) for a nucleus with spin $I \geq 1$ is obtained multiplying q_i (au) by 234.9647 times the nuclear quadrupole moment *Q* (barns).[28]

A previous discussion[28] on the *q* (nqcc) values of X/X^+ and XH/XH^+ pairs has shown that corresponding experimental values were well reproduced by our calculation methods, and in the absence of any literature results to compare with, the same trend is expected here for the XH^{2+} ions.

Excluding FH^{2+}, halogen q_0(X) is smaller in $XH^{2+}(\sigma^2\pi^2)$ than in XH($\sigma^2\pi^4$); that is, the asymmetry of the CDD at nucleus X is reduced upon double-ionization $\pi^2 \rightarrow \infty$ (Table 6). The opposite behavior is found for XH^+, where q_2(X) of $X^2\Pi$ [or q_0(X) in $A^2\Sigma^+$] is about 2.5 times larger than q_0(X) in XH; that is, the CDD(X) asymmetry increases upon single-ionization, $\pi \rightarrow \infty$ or $\sigma \rightarrow \infty$.

The q_i(H)'s lie below 0.6 au, resulting in $eQq_i(D) < 0.5$ MHz for all XH^{n+} ions, to be compared with halogen nqcc's of 60 MHz (^{35}Cl) and 370 MHz (^{79}Br). Such small nqcc(H)'s are understandable since the efg asymmetry at H, with no valence *p*-AO's of its own, is actually created by atom X, via its nuclear charge and *p*(X) orbitals. Not surprisingly, neutral FD exhibits the largest experimental eQq_0 for a D-containing species (340 ± 40 kHz),[28] due to the influence of the most electronegative F atom. The parallel q_0(H/D) values follow a simple trend: (i) largest for XH, 0.23−0.56 au; (ii) medium-large for $X^2\Pi(XH^+)$, 0.18−0.26 au; and (iii) very small for $A^2\Sigma^+(XH^+)$ and $X^3\Sigma^-(XH^{2+})$, up to 0.11 au.

A comparison in each metastable dication between magnetic and electric hfs's for $X^3\Sigma^-(XH^{2+})$ reveals that A_{dip}(X) and *eQq*(X) are of similar magnitude, as pointed out by A_{dip}/eQq values (in MHz) of about −86/-59 for ^{35}Cl and of −400/368 for ^{79}Br (Tables 6 and 7). This feature implies that fitting of experimental hf data on XH^{2+} ($X^3\Sigma^-$) requires a Hamiltonian in which both magnetic and electric terms are included. The same situation applies to the hyperfine spectra of XH^+ ions.[28]

3.4. Zero-Field Splitting (zfs): Splitting Constant λ. The spin−spin operator describes the interaction between (electron-spin) magnetic moments involving unpaired electrons.[26,44,45] In a two-electron open-shell state like $^3\Sigma^-(\pi^2)$, such interaction results in the S_z spin-component $S_0 = 2^{-1/2}(\alpha\beta+\beta\alpha)$ being more stable than the two degenerate spin-components $S_1 = \alpha\alpha$ and $S_{-1} = \beta\beta$. The energy separation $\Delta E_T = E(^3\Sigma^-\pm1) - E(^3\Sigma^-_0)$ is reported by experimentalists as 2λ, where λ is the so-called spin−spin fine structure constant. Up to 2nd-order, λ is the sum of two terms, λ_{SS}(1st) + λ_{SO}(2nd). Studies in the literature[26,44,45] have shown that λ_{SS}(1st) is of a few cm^{-1} in first-row atoms but negligibly small in heavier atoms, i.e., compared with λ_{SO}(2nd). The 2nd-order contribution to 2λ of a $X^3\Sigma^-$ state is given by the cumulative contribution of three different sum-over-states (SOS's), namely $2\lambda_{SO}[X^3\Sigma^-] = \Sigma_n\, S^2E(n^1\Sigma^+) + \Sigma_n\, S^2E(n^3\Pi) - \Sigma_n\, S^2E(n^1\Pi)$, where $S^2E(n^1\Sigma^+)$ stands for $|\langle X^3\Sigma^- |SO| n^1\Sigma^+\rangle|^2 \times [E(n^1\Sigma^+) - E(X^3\Sigma^-)]^{-1}$, etc. The $2\lambda_{SO}[X^3\Sigma^-]$ value is dominated by the coupling with $n^1\Sigma^+$ states, as the contributions from triplet and singlet Π states partially cancel each other (their total contribution should be small and positive).[45]

The calculated D_{SO} (= $2\lambda_{so}$) values are listed in Table 8, together with SO and ΔE data for $1^1\Sigma^+$, $1^3\Pi$, and $1^1\Pi$. Each zfs is here governed by the coupling between the $\sigma^2\pi^2$ states $X^3\Sigma^-$ and $1^1\Sigma^+$, which represents about 72% for FH^{2+} to 97% for ClH^{2+}/BrH^{2+}. The cumulative contribution from other states is less than 1 cm^{-1}. D_{SO} increases by 1 order of magnitude between FH^{2+} and ClH^{2+}, and between ClH^{2+} and BrH^{2+}. The first increase is due to a larger SO and a smaller ΔE in the Cl-dication, whereas the second is mainly caused by the large SO(Br) value.

A D_{SO} = 23 cm^{-1} for $ClH^{2+}(X^3\Sigma^-)$ estimated[4] from experimental PH/SH^+ data is quite realistic compared with 20.4 cm^{-1} calculated here (which is expected to be ca. 10% too small because of underestimated SO values).[28] Our D_{SO}'s for ClH^{2+} and BrH^{2+} are also in good agreement with recent experimental and/or theoretical results (see footnotes in Table 7).[3,16,17]

3.5. Electron-Spin Magnetic Moments (*g*-Factors) and Spin-Rotation Constants (γ). *3.5.1. Electron-Spin g-Factors.* The *g*-shift components calculated for $X^3\Sigma^-$ are summarized in Table 9. The *g*-shift is defined as $\Delta g = g - g_e$, where g_e = 2.002319 is the free-electron *g*-value (also known as g_S). For linear Σ radicals, the *g*-factor (or shift) is specified by both the parallel and perpendicular components. In a perturbation theory description (up to second-order), each Δg component is given by the sum of 1st and 2nd order contributions. Here, the 1st-order term (negative and not higher than 500 ppm in magnitude) is evaluated using ROHF($X^3\Sigma^-$) wave functions,[46] whereas 2nd-order terms for $X^3\Sigma^-$ are given by the SOS expansions $\Delta g_{||}$(2nd) = Σ_n SLE($n^3\Sigma^+$) and $\Delta g_\perp$(2nd) = Σ_n SLE($n^3\Pi$). In these expressions, SLE stands for the product SO×L×ΔE^{-1} (similar to that used for calculating zfs's, section 3.4), and *L* is the transition magnetic moment between $X^3\Sigma^-$ and $n^3\Sigma^+/n^3\Pi$ excited states.

The MRDCI data for the perpendicular *g*-shifts (Table 9) are obtained including 6 VEs as well as inner shells in the correlation treatment of 2nd order SOSs. For $\Delta g_{||}$, however, only 1st-order terms are considered since those for the 2nd-order coupling $X^3\Sigma^- - n^3\Sigma^+$ should be negligibly small, due to high ΔE and small *L*.[46] One MRDCI (6 VEs) calculation for the $X^3\Sigma^-(\sigma^2\pi^2) - 1^3\Sigma^+(\sigma\pi^2\sigma^*)$ coupling in ClH^{2+} gives ΔE, *L*, and SO

TABLE 8: Zero-Field Splitting of $X^3\Sigma^-$ States in XH^{2+}, as Given by the 2nd Order Parameter $D_{so} = 2\lambda$ (in cm^{-1}) and MRDCI Data, Including SO (cm^{-1}) and ΔE (eV) for Relevant Coupled States

radical	$D_{so}(1^1\Sigma^+)$ (SO/ΔE)	$D_{so}(1^3\Pi)$ (SO/ΔE)	$D_{so}(1^1\Pi)$ (SO/ΔE)	$^1\Sigma^+/^3\Pi/^1\Pi$[a] D_{so}	D_{so} (2nd) (total)
FH^{2+} (6e)	2.46	1.27	−0.52	0.17/0.03/−0.04	3.37
	(295.2/4.39)	(152.8/2.29)	(143.0/4.92)		
ClH^{2+} (6e)	17.70	2.70	−2.07	0.12/0.44/−0.51	18.38
	(653.0/2.99)	(269.8/3.34)	(279.2/4.67)		
(12e)	19.57	3.04	−2.32	0.14/0.46/−0.51	20.38[b]
	(683.7/2.96)	(285.3/3.32)	(295.3/4.66)		
BrH^{2+} (6e)	306.90	37.19	−31.42	1.22/7.59/−9.37	312.11
	(2619.5/2.77)	(1031.7/3.55)	(1088.2/4.67)		
(22e)	353.15	45.84	−36.97	1.30/9.12/−9.86	362.58 [c]
	(2802.9/2.76)	(1140.2/3.52)	(1177.6/4.65)		

[a] Cumulative contributions to D_{so} from higher lying $^1\Sigma^+$, $^3\Pi$, and $^1\Pi$ states. [b] Relativistic calculations[16b] find $2\lambda = 24.2$ cm^{-1} (3 meV). [c] Expt.: 445 ± 80 cm^{-1} (55 ± 10 meV),[3a] Auger spectrum; 379 cm^{-1} (47 meV)[3b] and 405 cm^{-1} (50 meV)[3c], both TPEsCO spectra. Theoretical: 387 cm^{-1} (48 meV), relativistic calculations.[17]

TABLE 9: Electron-Spin *g*-Shifts (ppm) and Curl's Spin-Rotation Constants γ (cm^{-1}) Calculated for $X^3\Sigma^-$ of XH^{2+} (X = F, Cl, and Br) (ROHF Data Used for 1st Order and MRDCI for 2nd Order Contributions)

XH^{2+}	$\Delta g_\perp$(2nd) $1^3\Pi$	(SO/*L*/ΔE)[a]	$\Delta g_\perp$[b] (n)$^3\Pi$	$\Delta g_\perp$ (1st)	$\Delta g_\perp$ (total)	$\Delta g_{\|\|}$ (1st)	$\langle\Delta g\rangle$[c]
FH^{2+} (6e)	16289	(152.8/0.983/2.29)	−100	−516	15670	−562	10250
ClH^{2+} (6e)	19087	(269.8/0.954/3.34)	−879	−276	17932[d]	−312	11850
(12e)	20340	(285.3/0.955/3.32)	−936	−276	19128[d]	−312	12650
γ[e]					−0.31[d]		
BrH^{2+} (6e)	67875	(1031.7/0.941/3.55)	−4918	−139	62818	−79	41850
(22e)	76097	(1140.2/0.946/3.52)	−5257	−139	70701	−79	47110
γ[f]					−0.98		

[a] SO in cm^{-1}, *L* in au, and ΔE in eV. [b] Cumulative contribution from higher $^3\Pi$ states. [c] Isotropic *g* shift, $\langle\Delta g\rangle = (2\Delta g_\perp + \Delta g_{\|\|})/3$. [d] See text for vibrationally averages. [e] $^{35}ClH^{2+}$ (12e results). [f] $^{79}BrH^{2+}$ (22e results).

values of 13.2 eV; 1.7×10^{-5} au and 15.2 cm^{-1}, respectively, resulting in $\Delta g_{\|\|}(2nd) \approx 10^{-9}$ (i.e., 5 orders of magnitude smaller than $\Delta g_{\|\|}(1st)$, Table 9).

Correlation of inner-shells leads to more accurate SO values, whereas *L* and ΔE change little (Table 9). The extended calculations give $\Delta g_\perp$'s of 19 130 ppm for ClH^{2+} and 70 700 ppm for BrH^{2+}, approximately 7 and 13% larger than with 6 VEs. Clearly, $\Delta g_\perp$ is governed in all cases by the coupling of $X^3\Sigma^-(\sigma^2\pi^2)$ with $1^3\Pi(\sigma\pi^3)$ where, as expected, the excitation $\sigma \rightarrow \pi$ of type DOMO (doubly occupied MO) → SOMO gives a positive contribution to $\Delta g_\perp$.

It is instructive to compare the $\langle\sigma^2\pi^2|$ SO $|\sigma\pi^3\rangle$ matrix element for $X^3\Sigma^-/1^3\Pi$ coupling in XH^{2+} with corresponding $\langle\sigma^2\pi^3|$ SO $|\sigma\pi^4\rangle$ for $X^2\Pi/1^2\Sigma^+$ in XH^+. Both can be formally reduced to a common matrix element $\langle\sigma|$ SO $|\pi\rangle$. For each of the series $FH^{n+} \rightarrow ClH^{n+} \rightarrow BrH^{n+}$, the SO values (in cm^{-1}) are 120.6, 250.4 and 1015.6 for n=1,[28] versus 152.8, 285.3 and 1140.2 for n=2 (Table 9). Contraction of the CDD upon ionization $XH^+ \rightarrow XH^{2+}$ is clearly reflected in the increased SO's for each XH^+/XH^{2+} pair. Most importantly, the spin−orbit constant $A(X^2\Pi) \propto |\langle\sigma^2\pi^3|SO|\sigma\pi^4\rangle|$ previously calculated for XH^+ using similar methods[28] reproduces quite well the experimental data (ours are about 6% smaller), and the same accuracy is expected for present $SO(XH^{2+})$ values.

The variations with *R* of SO, *L*, and $\Delta g_\perp$ were studied for $X^3\Sigma^-(ClH^{2+})$ since experimental evidence indicates that the effective *g*-factor changes drastically with vibrational excitation. This was assumed[5] to result from $\langle X^3\Sigma^-|$ SO $|1^3\Pi\rangle$ depending strongly on *R*. Our main results are shown graphically in Figures 4 and 5, where SO and *L* are $\sqrt{2}$ times the corresponding Cartesian values. The absolute value |SO| grows by about 10% between $R = \infty$ and $R \approx 3.1$ bohr, which we interpret as being caused by admixture of $Cl^{2+}H^0$ (with larger $\langle r^{-3}\rangle_{Cl}$) in the wave functions. On the other hand, *L* changes very little, practically retaining its asymptotic value $\langle 3p_\sigma\text{-Cl}|\ L\ |3p_\pi\text{-Cl}\rangle = \sqrt{2}$ at short *R*, that is, $3p_\sigma$-Cl mixes only slightly with 1s-H.

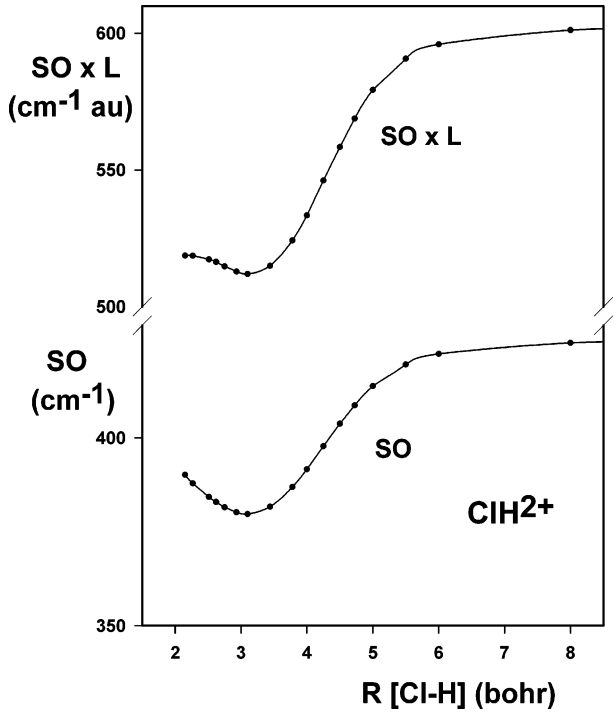

Figure 4. SO and SO×L values between $X^3\Sigma^-$ and $1^3\Pi$ of ClH^{2+} as a function of bond length (MRDCI, correlating 6 electrons).

$\Delta g_\perp$ shows a regular, steadily increasing behavior as *R* increases (Figure 5), in contrast to the nonstandard profile of the $X^3\Sigma^-$ potential (Figure 1). Up to about 3 bohr, the variation is practically linear, whereas thereafter it grows rapidly (mostly caused by the decrease of $\Delta E(^3\Sigma^- - 1^3\Pi)$). Selected $\Delta g_\perp$ values at $R = 2.4$, 3.1, 3.4, and 4.0 bohr are 15 300, 22 300, 27 000, and 43 400 ppm, respectively. The vibrationally averaged $\Delta g_\perp$'s are 18 550, 20 570, and 23 520 ppm for $v = 0$, 1, and 2, respectively. The data correlating 12 electrons should be about 7% larger (as suggested by the results in Table 9), so that our

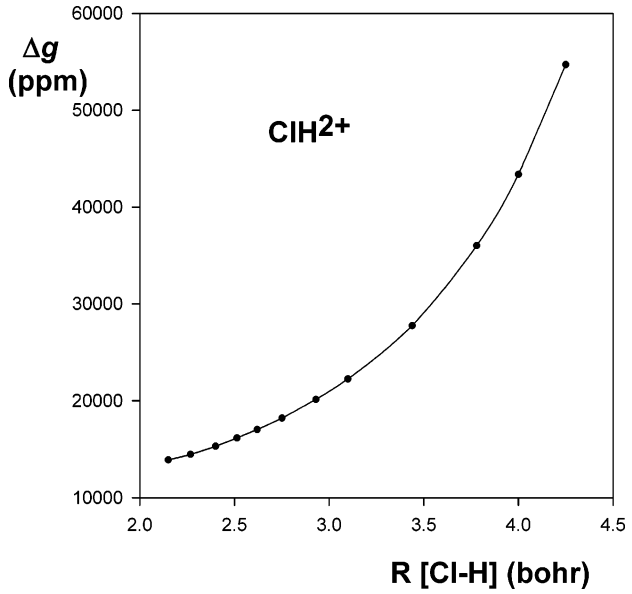

Figure 5. Total 2nd-order $\Delta g_\perp$-values of ClH^{2+} as a function of bond length. (MRDCI, correlating 6 electrons).

best $\Delta g_\perp(v)$ estimates, in ppm, are 19 850 for $v = 0$, 22 000 for $v = 1$, and 25 200 for $v = 2$.

3.5.2. Spin-Rotation Coupling Constants. Curl's expression, $\Delta g_\perp = -\gamma/2B$, states that the perdendicular g shift and γ constant are proportional to each other.[47] Since the rotational constant B is easily accessible from experimental or theoretical studies, one can estimate $\Delta g_\perp$ knowing γ, or vice versa. Adjusting B_e data[30] for the neutral pairs $^{35}ClH/^{35}ClD$ and $^{79}BrH/^{79}BrD$ by the $R_e(X^3\Sigma^-, XH^{2+})$ values from Table 1, one obtains B's (cm^{-1}) of 8.114/4.174 and 6.932/3.477 for the respective XH^{2+} ions. The total 2nd-order Δg's (Table 9) lead to Curl γ's of -0.31 cm^{-1} in $^{35}ClH^{2+}$ and -0.98 cm^{-1} in $^{79}BrH^{2+}$. Considering vibrational dependency, the best $\Delta g_\perp(v)$ estimates for $^{35}ClH^{2+}$ give γ_v's of -0.32, -0.36, and -0.41 cm^{-1} for $v = 0-2$. Further, γ's are -0.16 cm^{-1} for $^{35}ClD^{2+}$ and -0.49 cm^{-1} for $^{79}BrD^{2+}$, i.e., about $(1/2)\gamma(XH^{2+})$. Abusen et al.[4] analyzed the $^{35}ClD^{2+}$ spectrum assuming $\gamma \approx -0.1$ cm^{-1}, which is ca. 60% smaller than calculated here. Obviously, their choice $\gamma < 0$ implies a positive $\Delta g_\perp$ value, as found by us.

4. Comparison with ClH^{2+} Experiments

Abusen et al. studied for $X^3\Sigma^-(ClH^{2+})$ its rotationally resolved infrared spectrum[48a] and magnetic hfs,[4] while Cox and McNab analyzed the Zeeman splitting (effective g factors),[5] the only experimental studies to date dealing with the hf/hfs of dications.[2] Infrared absorption was assigned to the $v = 2 \leftarrow 1$ band.[20b] The hfs-resolved infrared spectra[4] of a $^PQ_{23}(N'')$ branch gave a Fermi contact constant b_F (A_{iso}) = 167(25) MHz for ^{35}Cl. The value of the dipole constant c could not be established (from -4 to $+204$ MHz for different combinations of $N'' = 7-11$). Later, Zeeman splittings were used to more accurately assign the spectrum as a $^PQ_{23}(6)$ fine structure transition.[5] Further analysis led to effective g values of 1.85 ± 0.05 for the lower (v,N,J) = (1,6,5) level and of 1.00 ± 0.04 for the upper (2,5,5) level. As said before, the authors related such (unusually) large difference in effective g's between two adjacent v levels to a strong dependence of $\langle X^3\Sigma^-|\ SO\ |1^3\Pi\rangle$ on R. The ($X^3\Sigma^-$) hf constants λ and γ were not determined in the mentioned papers. The analysis of the spectrum was done fixing $\lambda = 11.5$ cm^{-1} and $\gamma = -0.1$ cm^{-1}. Our calculated values are 10.2 and -0.16 cm^{-1} ($^{35}ClD^{2+}$), respectively. Other hyperfine interactions, nqcc's (eQq), A_{iso}, and A_{dip} for H/D isotopes, were not resolved either (to our understanding, zero values were assigned to them in their fitting hyperfine Hamiltonian).

Two main points of dissent arise regarding the above three articles. First, the c constant is reported to be positive, which seems to be incorrect. According to experimental studies on XH radicals with π-type SOMOs (and all σ-MO's closed), the c(X) constant describing the axial dipole−dipole interaction is negative (as long as the nuclear magnetic moment $\mu > 0$), as found for c(X) in the $X^2\Pi(\sigma^2\pi^3)$ state of $FH^+/ClH^+/BrH^+$ ions[28] or in the $X^3\Sigma^-(\sigma^2\pi^2)$ state of NH, PH, and AsH species.[49] In all examples where the maximum of the SDD is perpendicular to the bond the dipolar tensor ($T_{xx} + T_{yy}$) is positive, and accordingly, $T_{zz} = -(T_{xx} + T_{yy})$ has to be negative.

Second, the strong dependence of $\langle X^3\Sigma^-|\ SO\ |1^3\Pi\rangle$ with R is difficult to reconcile with $X^3\Sigma^-$ being mostly $\sigma^2\pi^2$ ($Cl^+ + H^+$) at all geometries (with some admixture of $\sigma\pi^2\sigma^*$ ($Cl^{2+} + H$) at short R) and $1^3\Pi(\sigma\pi^3)$ mainly retaining its asymptotic structure ($Cl^+ + H^+$) at all R's (small $\Delta E_{el}(1^3\Pi)$, Table 2). Since a similarly weak R-dependence holds for L, one concludes that any sizable variation of $\Delta g_\perp$ ($= SO \times L \times \Delta E^{-1}$) for the $X^3\Sigma^- - 1^3\Pi$ coupling should relate to ΔE. Obviously, the value of $\Delta E = [E(1^3\Pi) - E(X^3\Sigma^-, v)]$ is larger for $v = 1$ than for $v = 2$, so that it should hold that $g_\perp(v = 2) > g_\perp(v = 1)$. Our best data lead to vibrationally averaged $g_\perp$-values of 2.02217, 2.02432, and 2.02752 for $v = 0-2$, respectively. ($g_{||}$ lies close to 2.00200 throughout, Table 9.) As said above, the experimental effective g-factors follow the opposite behavior (they decrease with v). At this moment, it is not clear to us whether such a trend results from the (angular-momentum coupling) factors relating our calculated absolute to the reported effective $g_\perp$-factors.

In a recent paper,[2] new experimental results on $^{35}ClD^{2+}/^{37}ClD^{2+}$ were sketchily presented. The new Cl-data include (i) for $^{37}ClD^{2+}$, $b_F = 140(21)$ MHz, $c = -75(21)$ MHz and eQq_0= undetermined and (ii) for $^{35}ClD^{2+}$, $b_F = 162(30)$ MHz, with both c and eQq_0 undetermined (using isotopic relations, $c(^{35}Cl)$ was estimated to be $\approx -90(25)$ MHz). These values are in better accord with our results, although no details were given, and it is puzzling what changes in the spin-Hamiltonian were done, if any, to revert the sign of c from positive in ref 4 to negative (correct) in the most recent publication.[2]

5. Summary and Concluding Remarks

This theoretical study reports fine and hyperfine parameters for metastable $X^3\Sigma^-$ of ClH^{2+} and BrH^{2+} (repulsive FH^{2+} is also considered for comparison purposes), including magnetic (A_{iso}, A_{dip}) and electric-quadrupole (eQq) coupling constants, zero-field splittings (λ), electron-spin magnetic moments (g-factors), and spin-rotation constants (γ). Experimental data are restricted to λ of BrH^{2+}/BrD^{2+}, $A_{iso}(^{35,37}Cl)$, and $A_{dip}(^{37}Cl)$ of ClD^{2+}, and the effective g-factors for the $v = 1,2$ levels of $^{35}ClH^{2+}$. No theoretical values were available before, except for the λ's of ClH^{2+}/BrH^{2+}.

Our calculations find $A_{iso} = 110(15)$ MHz and $A_{dip} = -86(1)$ MHz for ^{35}Cl in ClH^{2+} vs 162 and -30 MHz, experimental.[2] Further, $\lambda = 363$ cm^{-1} calculated here for BrH^{2+} compares well with a relativistic result (387 cm^{-1}),[17] both values being somewhat smaller than 445 ± 80 cm^{-1}, experimental.[3] Our best estimates for $g_\perp(v)$ of ClH^{2+} are 2.02217, 2.02432, and 2.02752 for $v = 0$, 1, and 2, respectively; that is, the electron-spin magnetic moment increases with vibrational excitation. Experimentally, the effective $g_\perp(v)$ varies from 1.85 for $v = 1$ to 1.00 for $v = 2$ (it is not clear to us whether such a decrease could

arise from differences in the (angular-momentum coupling) factors, not specified in the original article,[5] affecting each hyperfine level). For BrH^{2+}, our best single-point calculation (Table 9) gives $g_\perp \approx 2.073$, which taking into account underestimation in the SO(Br) matrix elements[28] would lead to a more realistic estimate of $g_\perp \approx 2.083$ (± 0.003). Making use of Curl's approximation, our best γ-values are -0.32 cm^{-1} for $^{35}ClH^{2+}$ and -1.10 cm^{-1} for $^{79}BrH^{2+}$.

As expected, the hfs values for the X atom in the $X^3\Sigma^-$ states of XH^{2+} (X = F, Cl, and Br) are close to those for the $X^+(+H^+)$ product in its ^3P state. The theoretical A_{iso}(H) data clearly indicate that metastable states arise by the mixing of the attractive $X^{2+}H^0$ structure with the (dominant) repulsive X^+H^+ charge distribution. This effect is also seen in the electronic stabilization parameter ΔE_{el}, which is large (2−3 eV) for metastable but smaller (≈1 eV) for other potentials, which are indeed repulsive but not as strongly as for a strict $1/R$ dependency (for which $\Delta E_{el} \approx 0$).

Interestingly, FH^{2+} is found to have a bound $1^5\Sigma^-$ state, like previously known for ClH^{2+} and BrH^{2+}, but with a dissociation energy (≈0.5 eV) substantially larger than for the other two dications. This quintet state also has a sizable A_{iso}(H) corresponding to about 25% s-H character, in line with its four-open shells configuration $\sigma\pi^2[^4S,X^{2+}]\sigma^*[^2S,H]$. Experimental detection of these quintets, via double-ionization from XH, would be very difficult if $X^1\Sigma^+$ (GS) were the parent neutral state (triple-excitation) but much less so if the valence, long-range $2(B,V)^1\Sigma^+$ state were the initial state (double-excitation and favorable Franck−Condon factors).

The present data give a complete description of the fs and hfs of the $X^3\Sigma^-$ states of ClH^{2+} and BrH^{2+}, with no other dications in the literature being described in such detail as done here. As a matter of fact, we have reported[28] for $X^2\Pi$ and $A^2\Sigma^+$ of FH^+, ClH^+, and BrH^+ the complete set of parameters for spin−orbit (A), Λ-doubling (p,q), spin-rotation coupling (γ), magnetic (a,b,c,d), and electric quadrupole (eQq) couplings and the g-factors for the orbitally degenerate $X^2\Pi$ state. The experimental data on XH^+ were well reproduced, and the same should apply to the present results.

It is expected that our results will be helpful for future high-resolution spectroscopy works on ClH^{2+} and particularly for the less studied BrH^{2+}. Now, experimentalists have at hand all needed structural parameters to carry out a global fitting of their recorded spectra. We found, for instance, that the nqcc's (eQq's) for the Cl and Br nuclei are of comparable magnitude to the corresponding dipolar A_{dip} terms; that is, both have to be included in the fitting spin-Hamiltonian (although the nqcc contribution was discarded by experimentalists when dealing with the ClH^{2+} hf spectra).[2,4]

Acknowledgment. The authors thank NSERC (Canada) for financial support.

References and Notes

(1) (a) Tsai, B. P.; Eland, J. H. D. *Int. J. Mass Spectrom. Ion Phys.* **1980**, *36*, 143. (b) Mathur, D.; Andersen, L. H.; Hvelplundt, P. H.; Kella, D.; Safvan, C. P. *J. Phys. B.: At. Mol. Opt. Phys.* **1995**, *28*, 3415. (c) Schröder, D.; Schwarz, H. *J. Phys. Chem. A* **1999**, *103*, 7385. (d) Price, S. D. *Phys. Chem. Chem. Phys.* **2003**, *5*, 1717. (e) Mathur, D. *Phys. Rep.* **2004**, *39*, 1.

(2) Cox, S. G.; Critchley, A. D.; Kreynin, P. S.; McNab, I. R.; Shiell, R. C.; Smith, F. E. *Phys. Chem. Chem. Phys.* **2003**, *5*, 663.

(3) (a) Püttner, R.; Hu, Y. F.; Bancroft, G. M.; Aksela, H.; Nõmmiste, E.; Karvonen, J.; Kivimäki, A.; Aksela, S. *Phys. Rev. A* **1999**, *59*, 4438. (b) Yencha, A. J.; Juarez, A. M.; Lee, S. P.; King, G. C. *Chem. Phys. Lett.* **2003**, *381*, 609. (c) Alagia, M.; Brunetti, B. G.; Candori, P.; Falcinelli, S.; Teixidor, M. M.; Pirani, F.; Richter, R.; Stranges, S.; Vecchiocattivi, F. *J. Chem. Phys.* **2004**, *120*, 6980 and 6985.

(4) Åbusen, R.; Bennett, F. R.; Cox, S. G.; McNab, I. R.; Sharp, D. N.; Shiell, R. C.; Smith, F. E.; Walley, J. M. *Phys. Rev. A* **2000**, *61*, 50501.

(5) Cox, S. G.; McNab, I. R. *J. Phys. B: At. Mol. Opt. Phys.* **2002**, *35*, L237.

(6) Dorman, F. H.; Morrison, J. D. *J. Chem. Phys.* **1961**, *35*, 575.

(7) Bruna, P. J.; Peyerimhoff, S. D. *Faraday Symp. Chem. Soc.* **1984**, *19*, 193.

(8) Gill, P. M. W.; Radom, L. *Chem. Phys. Lett.* **1988**, *147*, 213; *J. Am. Chem. Soc.* **1989**, *111*, 4613.

(9) Moore, C. E. *Atomic Energy Levels*; NSRDS−NBS Circular No 35; U.S. Government Printing Office: Washington, DC, 1971.

(10) (a) Shaw, R. W.; Thomas, T. D. *Phys. Rev.* A **1975**, *11*, 1491. (b) Hitchcock, A. P.; Brion, C. *J. Phys. B*: *At. Mol. Phys.* **1981**, *14*, 4399. (c) Svensson, S.; Karlsson, L.; Märtensson, N.; Baltzer, P.; Wannber, B. *J. Electron Spectrosc. Relat. Phenom.* **1990**, *50*, C1.

(11) (a) Fægri, K. *Chem. Phys. Lett.* **1977**, *46*, 541. (b) Kvalheim, O. M.; Fægri, K. *Chem. Phys. Lett.* **1979**, *67*. 127. (c) Fægri, K.; Kelly, H. P. *Phys. Rev. A* **1979**, *19*, 1649. (d) Zähringer, K.; Meyer, H.-D.; Cederbaum, L. S. *Phys. Rev. A* **1992**, 45, 318. (e) Schimmelpfennig, B.; Nestmann, B. M.; Peyerimhoff, S. D. *J. Electron Spectrosc. Relat. Phenom.* **1995**, *174*, 173.

(12) Fournier, P. G.; Mousselmal, M.; Peyerimhoff, S. D.; Banichevich, A.; Adam, M. Y.; Morgan, T. J. *Phys. Rev. A* **1987**, *36*, 2594.

(13) Svensson, A.; Hughes, E. A.; Banichevich, A.; Peyerimhoff, S. D.; Hess, B. A. *J. Phys. B.: At. Mol. Opt. Phys.* **1991**, *24*, 2997.

(14) Banichevich, A.; Peyerimhoff, S. D.; van Hemert, M. C.; Fournier, P. G. *Chem. Phys.* **1988**, *121*, 351.

(15) Banichevich, A.; Peyerimhoff, S. D.; Hess, B. A.; van Hemert, M. C. *Chem. Phys.* **1991**, *154*, 199.

(16) (a) Fink, R. F.; Kivilompolo, M.; Aksela, H.; Aksela, S. *Phys. Rev. A* **1998**, *58*, 1988. (b) Ellingsen, K.; Matila, T.; Saue, T.; Aksela, H.; Gropen, O. *Phys. Rev. A* **2000**, *62*, 032502.

(17) Matila, T.; Ellingsen, K.; Saue, T.; Aksela, H.; Gropen, O. *Phys. Rev. A* **2000**, *61*, 032712.

(18) (a) Aksela, H.; Aksela, S.; Hotokka, M.; Jäntti, M *Phys. Rev. A* **1983**, *28*, 287. (b) Kvalheim, O. M. *Chem. Phys. Lett.* **1983**, *98*, 457. (c) Karlsson, L.; Baltzer, P.; Svensson, S.; Wannberg, B. *Phys. Rev. Lett.* **1988**, *60*, 2473. (d) Svensson, S.; Karlsson, L.; Baltzer, P.; Keane, M. P.; Wannberg, B. *Phys. Rev. A* **1989**, *40*, 4369. (e) McConkey, A. G.; Dawber, G.; Avaldi, L.; MacDonald, M. A.; King, G. C.; Hall, R. I. *J. Phys. B: At. Mol. Opt. Phys.* **1994**, *27*, 271. (f) Yencha, A. J.; King, G. C.; Lopes, M. C.; Bozek, J. D.; Berrah, N. *Chem. Phys. Lett.* **1999**, *315*, 37. (g) Critchley, A. D. J.; King, G. C.; Kreynin, P.; Lopes, M. C. A.; McNab, I. R.; Yencha, A. J. *Chem. Phys. Lett.* **2000**, *349*, 79. (h) Harper, S.; Calandra, P.; Price, S. D. *Phys. Chem. Chem. Phys.* **2001**, *3*, 741. (i) Alagia, M.; Biondini, F.; Brunetti, B. G.; Candori, P.; Falcinelli, S.; Teixidor, M. M.; Pirani, F.; Richter, R.; Stranges, S.; Vecchiocattivi, F. *J. Chem. Phys.* **2004**, *121*, 10508.

(19) (a) Shaw, D. A.; Cvejanović, D.; King, G. C.; Read, F. H. *J. Phys. B: At. Mol. Phys.* **1984**, *17*, 1173. (b) Wannberg, W.; Svensson, S.; Keane, M. P.; Karlsson, L.; Baltzer, P. *Chem. Phys.* **1989**, *133*, 281. (c) Alagia, M.; Boustimi, M.; Brunetti, B. G.; Candori, P.; Falcinelli, S.; Richter, R.; Stranges, S.; Vecchiocattivi, F. *J. Chem. Phys.* **2002**, *117*, 1098 (see also comment[4] in ref 3c). (d) Eland, J. H. D. *Chem. Phys.* **2003**, *294*, 171.

(20) (a) Olsson, B. J.; Larsson, M. *J. Phys. B: At. Mol. Phys.* **1987**, *20*, L137. (b) Bennett, F.; McNab, I. R. *Chem. Phys. Lett.* **1996**, *251*, 405. (c) Teixidor, M. M.; Pirani, F.; Candori, P.; Falcinelli, S.; Vecchiocattivi, *Chem. Phys. Lett.* **2003**, *379*, 139.

(21) Pope, S. A.; Hillier, I. H.; Guest, M. F. *Faraday Symp. Chem. Soc.* **1984**, *19*, 109.

(22) Nefedova, V. V.; Boldyrev, A. I.; Simons, J. *Int. J. Quantum Chem.* **1995**, *55*, 441.

(23) Lushington, G. H.; Bruna, P. J.; Grein, F. *Z. Phys. D*: *At. Mol. Clusters* **1996**, *36*, 301.

(24) Frisch, M. J.; et al. *Gaussian 03*, Rev. B.04; Gaussian Inc.: Pittsburgh, PA, 2003.

(25) (a) Buenker, R. J.; Peyerimhoff, S. D.; Butscher, W. *Mol. Phys.* **1978**, *35*, 771. (b) Buenker, R. J., in *Studies in Physical and Theoretical Chemistry*. *Current Aspects of Quantum Chemistry*; Carbó, R., Ed.; Elsevier: Amsterdam, 1982; Vol. 21. (c) Marian, C. M. Ph.D. Thesis, University of Bonn: Bonn, Germany, 1981. (d) Hess, B. A. Ph.D. Thesis, University of Bonn: Bonn, Germany, 1981. (e) Chandra, P.; Buenker, R. J. *J. Chem. Phys.* **1983**, *79*, 358.

(26) Hess, B. A.; Marian, C. M. Relativistic Effects in the Calculation of Electronic Energies. In *Computational Molecular Spectroscopy*; Jensen, P., Bunker, P. R., Eds.; Wiley: New York, 2000; pp 169.

(27) Bruna, P. J.; Peyerimhoff, S. D. *Adv. Chem. Phys.* **1987**, *67*, 1.

(28) Bruna, P. J.; Grein, F. *Mol. Phys.* **2006**, *104*, 429.

(29) Luzanov, A. V.; Babich, E. N.; Ivanov, V. V. *J. Mol. Struct. (THEOCHEM)* **1994**, *311*, 211.

(30) (a) Huber, K. P.; Herzberg, G. *Molecular Spectra and Molecular Structure: IV. Constants of Diatomic Molecules*; Van Nostrand: New York,

1979. (b) Di Lonardo, G.; Douglas, A. E. *Can. J. Phys.* **1973**, *51*, 434. (c) Ginter, D. S.; Ginter, M. L.; Tilford, S. G. *J. Mol. Spectrosc.* **1981**, *90*, 152. (d) Ginter, D. S.; Tilford, S. G. *J. Mol. Spectrosc.* **1981**, *90*, 177.

(31) (a) Bruna, P. J.; Hirsch, G.; Buenker, R. J.; Peyerimhoff, S. D. In *Molecular Ions: Geometric and Electronic Structures*; Berkowitz, J., Groneveld, K.-O., Eds.; NATO ASI Series B: Physics, Vol. 90; Plenum Press: New York, 1983; p 309. (b) Bettendorf, M.; Peyerimhoff, S. D.; Buenker, R. J. *Chem. Phys.* **1982**, *66*, 261. (c) Bettendorf, M.; Buenker, R. J.; Peyerimhoff, S. D.; Römelt, J. *Z. Phys. A: Atoms Nuclei* **1982**, *304*, 125.

(32) (a) Bruna, P. J.; Wright, J. S. *J. Chem. Phys.* **1990**, *93*, 2617. (b) Bruna, P. J.; Di Labio, G. A.; Wright, J. S. *J. Phys. Chem.* **1992**, *96*, 6269. (c) Bruna, P. J.; Wright, J. S. *J. Phys. B: At. Mol. Opt. Phys.* **1993**, *26*, 1819. (d) Mawhinney, R. C.; Bruna, P. J.; Grein, F. *J. Phys. B: At. Mol. Opt. Phys.* **1995**, *28*, 4015. (e) Mawhinney, R. C.; Bruna, P. J.; Grein, F. *J. Chem. Phys.* **1995**, *103*, 8948. (f) Bruna, P. J.; Mawhinney, R. C.; Grein, F. *Int. J. Quantum Chem. Symp.* **1995**, *29*, 455.

(33) Huang, Z.; Zhu, Z. H. *J. Mol. Struct.* **2000**, *525*, 123.

(34) Weltner, W. *Magnetic Atoms and Molecules*; Dover: New York, 1983.

(35) Fitzpatrick, J. A. J.; Manby, F. R.; Western, C. M. *J. Chem. Phys.* **2005**, *122*, 084312.

(36) (a) Harvey, J. S. M. *Proc. R. Soc. London, Ser. A* **1964**, *285*, 581. (b) Schaefer, H. F.; Klemm, R. A.; Harris, F. E. *Phys. Rev.* **1968**, *176*, 49. (c) Schaefer, H. F.; Klemm, R. A.; Harris, F. E. *Phys. Rev.* **1969**, *181*, 137. (d) Hay, P. J.; Goddard, W. A. *Chem. Phys. Lett.* **1971**, 9, 356. (e) Larsson, S.; Brown, R. E.; Smith, V. H. *Phys. Rev. A* **1972**, *6*, 1375.

(37) (a) King, J. G.; Jaccarino, V. *Phys. Rev.* **1954**, *94*, 1610. (b) Brown, H. H.; King, J. G. *Phys. Rev.* **1966**, *142*, 53. (c) Bagus, P. S.; Liu, B.; Schaefer, H. F. *Phys. Rev. A* **1970**, *2*, 555. (d) Altan Uslu, K.; Code, R. F.; Harvey, J. S. M. *Can. J. Phys.* **1974**, *52*, 2135.

(38) (a) Goodings, D. A. *Phys. Rev.* **1961**, *123*, 1706. (b) Desclaux, J. P.; Bessis, N. *Phys. Rev. A* **1970**, *2*, 1623. (c) Luc-Koenig, E.; Morillon, C.; Vergès, J. *Physica* **1973**, *70*, 175. (d) Bhat, S. V.; Weltner, W. *J. Chem. Phys.* **1980**, *73*, 1498.

(39) Lucken, E. A. C. *Nuclear Quadrupole Coupling Constants*; Academic Press: London, 1969.

(40) Fraga, S.; Karwoski, J.; Saxena, K. M. *Handbook of At. Data*; Elsevier: Amsterdam, 1976.

(41) Richards, W. G.; Trivedi, H. P.; Cooper, D. L. *Spin−orbit Coupling in Molecules*; International Series of Monographs in Chemistry; Clarendon Press: Oxford, 1981.

(42) Engels, B.; Eriksson, L. A.; Lunell, S. *Adv. Quantum Chem.* **1996**, *27*, 298.

(43) Frosch, R. A.; Foley, H. M. *Phys. Rev.* **1952**, *88*, 1337.

(44) (a) Hirota, E. *High-Resolution Spectroscopy of Transient Molecules*; Springer: Berlin, 1985. (b) Brown, J.; Carrington, A. *Rotational Spectroscopy of Diatomic Molecules*; Cambridge University Press: Cambridge, 2003.

(45) (a) Kayama, K.; Baird, J. C. *J. Chem. Phys.* **1967**, *46*, 2604. (b) Horani, M.; Rostas, J.; Lefebvre-Brion, H. *Can. J. Phys.* **1967**, *45*, 3319. (c) Palmiere, P.; Sink, M. L. *J. Chem. Phys.* **1976**, *65*, 3641. (d) Langhoff, S. R.; Kern, C. W. In *Modern Theoretical Chemistry*; Schaefer, H. F., Ed.; Plenum Press: New York, 1977. (e) Lefebvre-Brion, H.; Field, R. W. *The Spectra and Dynamics of Diatomic Molecules*; Elsevier: Amsterdam, 2004.

(46) (a) Lushington, G. H. Ph.D. Thesis, University of New Brunswick: New Brunswick, Canada, 1996. (b) Lushington, G. H.; Grein, F. *Theor. Chim. Acta* **1996**, *93*, 259. (c) Lushington, G. H.; Grein, F. *Int. J. Quantum Chem. Symp.* **1996**, *60*, 1679. (d) Lushington, G. H.; Grein, F. *J. Chem. Phys.* **1997**, *106*, 3292.

(47) Curl, R. F. *Mol. Phys.* **1965**, *5*, 585.

(48) (a) Abusen, R.; Bennett, F. R.; McNab, I. R.; Sharp, D. N.; Shiell, R. C.; Woodward, C. A. *J. Chem. Phys.* **1998**, *108*, 1781. (b) Bennett, F. R.; Critchley, A. D.; King, G. C.; LeRoy, R. J.; McNab, I. R. *Mol. Phys.* **1999**, *97*, 35.

(49) (a) NH: Ubachs, W.; Ter Meulen, J. J.; Dymanus, A. *Can. J. Phys.* **1984**, *62*, 1374. (b) PH: Klisch, E.; Klein, H.; Winnewisser, G.; Herbst, E. *Z. Naturforsch.* **1998**, *53a*, 733. (c) AsH: Fujiwara, H.; Kobayashi, K.; Ozeki, H.; Saito, S.; Jaman, A. I. *J. Chem. Soc. Faraday Trans.* **1997**, *93*, 1045 and references therein.